POLITECNICO DI TORINO

Master's Degree in Biomedical Engineering

Master Degree Thesis

Organ-on-chip based dynamic 3D breast cancer model for investigating glucose restriction as an adjuvant to chemotherapy

Supervisors

Prof. Gianluca CIARDELLI

Dr. Silvia SCAGLIONE

Dr. Elisabetta PALAMÀ

Candidate

Andrea GIANNOCCARO

A.A 2023\2024

Abstract

Triple-negative breast cancer (TNBC) represents one of the major cancer clinical challenges due to its aggressive nature and lack of targeted therapies. This is also due to poor predictive human breast cancer experimental models to be used to deepening drug resistance mechanisms and metastatic progression. Recently, traditional therapeutic approaches have been combined to specific diet restrictions, and some clinical trials are running. This study aims to develop a novel 3D *in vitro* TNBC model integrated into an organ-on-chip platform to evaluate the impact of glucose restriction on breast cancer cells viability and chemotherapy efficacy.

MDA-MB-231 cells were embedded in tunable alginate-based hydrogels and cultured dynamically using the MIVO® organ-on-chip platform, replicating the *in vivo* systemic drug diffusion. Tumor models were exposed to normal, restricted, and fasting glucose conditions (normal: 25 mM, restricted: 5 mM, and fasting: 0 mM), as well as combined fasting and chemotherapy treatments (10 µM of cisplatin) resembling plasma drug concentration. A healthy cellular control model with human dermal fibroblasts (HDFs) was used to assess off-target effects. Comparative analyses were performed under static and dynamic culture conditions, focusing on cell viability (dead alive assay), metabolic activity (Alamar blue), and cellular morphology. Immunostaining was employed to evaluate cell proliferation (Ki67) and hypoxia (HIF-1α) as key indicators of tumor cells behavior under varying glucose and treatment conditions.

In 2D cultures, glucose restriction did not significantly affect tumor cell viability, whereas complete glucose deprivation led to a 50% reduction in tumor cell viability after three days, irrespective of FBS serum concentration in the medium (10-5-2%), with minimal effects observed in healthy control cells as reported *in vivo*. Interestingly, in glucose deprivation condition, 3D cells culture viability was slightly higher, at approximately 65% in both static and dynamic conditions, likely due to the protective effect of the alginate matrix. The organ on chip based dynamic culture system significantly enhanced drug diffusion and cisplatin efficacy compared to static conditions (60% cells viability in static vs. 30% in dynamic), aligning more closely with clinical observations. Combined fasting and chemotherapy treatments resulted in a decrease in tumor viability; however,

immunostaining showed that cells remained positive for both Ki67 and HIF-1α, indicating ongoing proliferation and hypoxia in the tumor microenvironment. These findings suggest that fasting and chemotherapy interactions require further investigation to clarify their combined effects.

In conclusion, this advanced 3d tumor model based on a organ on chip culture represents a robust, scalable, and predictive tool for studying tumor biology, evaluating combined therapeutic strategies, and investigating tumor cell-matrix interactions. By enabling drug efficacy screening and facilitating the exploration of metabolic dependencies in a more controlled and biomimetic *in vitro* environment, it may be possible to bridge critical gaps in translational oncology, ultimately enhancing the reliability of preclinical models.

Keywords: breast cancer, glucose restriction, chemotherapy, *in vitro* model, 3D dynamic culture, Organ-on-chip.

Abstract in lingua italiana

Il tumore al seno triplo negativo (TNBC) rappresenta una delle principali sfide cliniche oncologiche a causa della sua natura aggressiva e della mancanza di terapie mirate. Questa difficoltà è ulteriormente accentuata dalla carenza di modelli sperimentali predittivi di carcinoma mammario umano, utili per approfondire i meccanismi di resistenza ai farmaci e la progressione metastatica. Recentemente, gli approcci terapeutici tradizionali sono stati combinati con specifiche restrizioni dietetiche, e sono attualmente in corso alcuni studi clinici. Questo studio si propone di sviluppare un innovativo modello *in vitro* 3D di TNBC integrato in una piattaforma organ-on-chip per valutare l'impatto della restrizione di glucosio sulla vitalità delle cellule tumorali e sull'efficacia della chemioterapia.

Le cellule MDA-MB-231 sono state incorporate in idrogel a base di alginato modulabile e coltivate in modo dinamico utilizzando la piattaforma organ-on-chip MIVO®, replicando la diffusione sistemica dei farmaci osservata *in vivo*. I modelli tumorali sono stati esposti a condizioni di glucosio normale, ristretto e nullo (normale: 25 mM, ristretto: 5 mM, nullo: 0 mM), così come a trattamenti combinati di digiuno e chemioterapia (10 µM di cisplatino), riproducendo le concentrazioni plasmatiche del farmaco. Un modello di controllo cellulare sano, costituito da fibroblasti dermici umani (HDF), è stato utilizzato per valutare gli effetti off-target. Sono state condotte analisi comparative in condizioni di coltura statica e dinamica, focalizzandosi sulla vitalità cellulare (saggio live/dead), sull'attività metabolica (AlamarBlue) e sulla morfologia cellulare. L'immunostaining è stato impiegato per valutare la proliferazione cellulare (Ki67) e l'ipossia (HIF-1α) come indicatori chiave del comportamento delle cellule tumorali in condizioni di glucosio variabile e trattamenti specifici.

Nelle colture 2D, la restrizione di glucosio non ha influenzato significativamente la vitalità delle cellule tumorali, mentre la completa deprivazione di glucosio ha portato a una riduzione del 5% della vitalità delle cellule tumorali dopo tre giorni, indipendentemente dalla concentrazione di siero FBS nel terreno di coltura (10-5-2%), con effetti minimi osservati nelle cellule sane di controllo, come riportato *in vivo*. È interessante notare che, in condizioni di deprivazione di glucosio, la vitalità delle colture 3D era leggermente superiore, attestandosi intorno al 65% sia in condizioni statiche che dinamiche, proba-

bilmente a causa dell'effetto protettivo della matrice di alginato. Il sistema di coltura dinamica basato su organ-on-chip ha migliorato significativamente la diffusione del farmaco e l'efficacia del cisplatino rispetto alle condizioni statiche (60% di vitalità cellulare in condizioni statiche contro il 30% in condizioni dinamiche), allineandosi maggiormente con le osservazioni cliniche. I trattamenti combinati di digiuno e chemioterapia hanno determinato una riduzione della vitalità tumorale; tuttavia, dall'immunostaining si è osservato che le cellule sono rimaste positive a Ki67 e HIF-1α, indicando una proliferazione e ipossia persistenti nel microambiente tumorale. Questi risultati suggeriscono che le interazioni tra digiuno e chemioterapia richiedono ulteriori approfondimenti per chiarire i loro effetti combinati.

In conclusione, questo avanzato modello tumorale 3D basato su una coltura organ-on-chip rappresenta uno strumento robusto, scalabile e predittivo per lo studio della biologia tumorale, la valutazione di strategie terapeutiche combinate e l'indagine sulle interazioni tra cellule tumorali e matrice extracellulare. Permettendo lo screening dell'efficacia dei farmaci e l'esplorazione delle dipendenze metaboliche in un ambiente *in vitro* più controllato e biomimetico, si potrebbero colmare lacune critiche nell'oncologia traslazionale e migliorare l'affidabilità dei modelli preclinici.

Parole chiave: carcinoma mammario, restrizione glucosio, chemioterapia, *in vitro* model, coltura 3D dinamica, Organ-on-chip.

Contents

1 | Introduction

1.1. Triple Negative Breast Cancer (TNBC)

1.1.1. Cancer and breast cancer

Cancer is a multifaceted and life-threatening condition, defined by the uncontrolled proliferation and dissemination of aberrant cells throughout the body. According to the National Cancer Institute, cancer is characterized as "a disease in which some of the body's cells grow uncontrollably and spread to other parts of the body" [1]. More precisely, cancer emerges from the transformation of normal cells, leading to clonal proliferation of these transformed cells, which undergo natural selection processes, thereby facilitating their adaptation and evolution. The global burden of cancer has been progressively escalating, rendering it one of the foremost causes of mortality worldwide [2]. Cancer-related mortality remains profoundly significant, positioning it as the second leading cause of death globally. Furthermore, population growth, aging, and the increasing adoption of cancer risk associated lifestyle behaviors contribute to a further worsening of future projections.

Among the various forms of cancer, breast cancer stands out as the most prevalent malignancy among women worldwide, representing a significant clinical challenge due to its molecular heterogeneity [3]. In 2018 alone, approximately one out of four cases of all cancer diagnosis in women were breast cancer-related. The clinical manifestation of breast cancer varies based on its molecular and histopathological characteristics, which critically determine both prognostic outcomes and therapeutic strategies. Early-stage breast cancer, which is typically confined to the breast and regional lymph nodes, is curable in approximately 70-80% of cases with timely and appropriate intervention. Conversely, advanced (metastatic) breast cancer remains mostly incurable, with therapeutic approaches primarily aimed at symptom relief and extending survival [3] Within the spectrum of breast cancer subtypes, triple-negative breast cancer (TNBC) is particularly aggressive and difficult to manage, making it one of the most challenging clinical issues in the last decades.

1.1.2. TNBC: characteristics and clinical overview

Triple-negative breast cancer is characterized by the absence of estrogen receptors (ER), progesterone receptors (PR), and the human epidermal growth factor receptor 2 (HER2). Overall, it represents a biologically diverse entity with intricate molecular characteristics. Therefore, at the molecular level, TNBC can be classified into several key subtypes, including basal-like 1 (BL1), basal-like 2 (BSL), mesenchymal, mesenchymal stem-like (MSL), immunomodulatory (IM), and luminal androgen receptor (LAR) subtypes [4, 5]. All these subtypes are characterized by distinct gene expression profiles that are directly linked to both their biological behavior and therapeutic responses. For instance, BL1 tumors are defined by high proliferative activity and enhanced DNA damage response, which make them relatively more susceptible to platinum-based chemotherapy. This molecular heterogeneity highlights the complexity of this tumor type underscoring the necessity for specific therapeutic strategies.

TNBC is clinically recognized for its aggressive nature, accounting for approximately 10-20% of all breast cancer. Moreover, in the first few years following diagnosis, high rates of recurrence and metastasis have been frequently observed [6]. The lack of receptors expression makes typical therapeutic strategies, such as targeted endocrine therapies, largely ineffective, resulting in limited treatment options for patients with TNBC. Chemotherapy remains indeed the primary systemic therapy for this specific tumor [5]. However, despite initial sensitivity to chemotherapy, a significant proportion of patients experience early relapses and disease progression, which contributes to poorer overall survival rates compared to other breast cancer subtypes [7]. Although chemotherapy remains the cornerstone of TNBC management, it is often insufficient as a curative option in advanced stages, emphasizing the critical need for more effective therapeutic approaches [8]. Recent advancements in TNBC treatment are based on newer drug like immune therapies, specific enzyme inhibitors, and other targeted drug combinations. However, many patients still do not achieve lasting remission, and resistance to available treatments remains a significant challenge.

The current treatment landscape underscores an urgent need for novel and effective therapies developed through innovative approaches to better address therapeutic resistance and improve patient outcomes. Exploring new methodologies to understand TNBC's molecular subtypes and the tumor microenvironment will be essential in guiding future therapeutic strategies.

1.2. Tumor microenvironment and metabolism

To fully understand tumors, they must be studied and observed as heterogeneous systems consisting of a specific microenvironment (tumor microenvironment, TME) and a complex and dynamic metabolism. In the tumor microenvironment of solid tumors, it is possible to distinguish a non-cellular component that predominantly includes the extracellular matrix (ECM), mainly composed of proteins, glycoproteins, and proteoglycans, which provides structural support and biomechanical signals to the tumor mass itself, and a cellular component [9, 10]. This is a complex and heterogeneous assembly of neoplastic and non-neoplastic cells, also referred to as the "stroma" [9, 11]. Among cell types composing the stroma are cancer-associated fibroblasts (CAFs), T cells, macrophages, neutrophils, and endothelial cells, as shown in Figure 1.1.

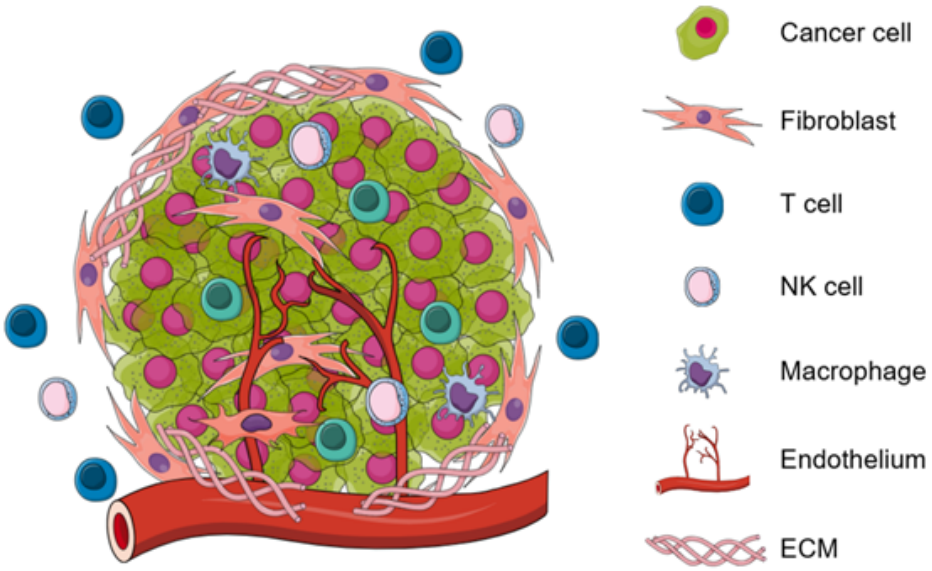

Figure 1.1: Illustration of tumor microenvironment, highlighting the dynamic interactions between malignant cells, cancer-associated fibroblasts, immune cells, and the extracellular matrix (ECM), which collectively influence tumor growth and progression. Edited on mindthegraph.com

Among the various cell populations that constitute the TME, metabolic interactions between malignant and healthy cells can be both symbiotic and competitive, as well as dynamic and heterogeneous [12–14]. Overall, tumor metabolism is highly dynamic and adaptable, influenced by a multitude of factors, including the availability of nutrients and oxygen within the tumor tissue itself. A determining factor is the variability in the distribution of endothelial vessels that vascularize the tumor, resulting in intratumoral metabolic heterogeneity. Regions with optimal perfusion gain access to alternative en-

ergy sources such as lipids and amino acids, while other poorly perfused areas primarily depend on glycolysis [9, 11]. The availability of essential resources for survival (glucose, fatty acids, glutamine, and oxygen) is thus limited [15]. A delicate balance of metabolic demands is therefore created, fostering both symbiotic and antagonistic competition between tumor cells and healthy cells within the microenvironment. One example of a symbiotic relationship is the behavior of cancer-associated fibroblasts (CAFs). Under nutritional stress, they support tumor cells by providing alternative nutrients such as lactate or alanine to fuel their accelerated metabolism [13, 15, 16]. Conversely, an antagonistic relationship exists between neoplastic cells and infiltrating immune cells, such as T lymphocytes. Both cell types primarily compete for the same resource, namely glucose. Tumor cells are generally characterized by accelerated glycolysis (Warburg effect) [17] and rapid glucose consumption, depriving T lymphocytes of it and impairing their effector function. T cells experience "metabolic exhaustion" that hinders their activation and production of cytokines such as interferon gamma (IFN-γ), necessary for the elimination of tumor cells [9, 15]. This may promote tumor growth and undermine anti-tumor immune responses.

1.2.1. Metabolic reprogramming in cancer

Tumor cells, beyond benefiting from the supporting TME, are generally endowed with a plastic metabolism. This metabolic flexibility enables them to thrive and sustain rapid growth even in nutritionally deprived conditions. To meet their proliferative demands, tumor cells dynamically adapt their metabolic processes, ranging from the upregulation of glucose metabolism to the utilization of lipids, amino acids, and mechanisms that maintain redox balance [16]. One of the main features of tumor metabolic reprogramming is the aforementioned "Warburg Effect," first described by the German physiologist and biochemist Otto Warburg. His pioneering reaserch into tumor cell metabolism revealed that, even in the presence of oxygen, cancer cells preferably rely on aerobic glycolysis over mitochondrial oxidative phosphorylation, which is the typical pathway for energy production in healthy cells under similar conditions [17]. Although less energy-efficient, this process converts glucose into pyruvate to generate ATP, while also providing essential intermediates for the biosynthesis of macromolecules (such as lipids, proteins, and nucleotides), needed to sustain the heightened proliferation of cancer cells. Additionally, pyruvate is converted into lactate (a hallmark of anaerobic glycolysis), despite oxygen availability, leading to acidification of the TME. These conditions within the tumor microenvironment overall promote tumor progression and immune evasion, further enhancing cancer's survival and growth strategies [15, 16]. Another crucial aspect of tumor metabolic reprogramming is

the de novo synthesis of fatty acids to meet the demand for new membrane components and cellular signaling molecules [16]. Fatty acid synthesis is indeed essential for tumor growth and is tightly regulated by key metabolic sensors, such as AMP-activated protein kinase (AMPK) and the mammalian target of rapamycin (mTOR), which orchestrate the balance between energy availability and cell growth. Similarly, glutamine metabolism plays an important role in the tumor environment. This amino acid is utilized both for indirect ATP production and as a nitrogen source for the biosynthesis of nucleotides and other essential metabolic intermediates [9]. Together, these metabolic adaptations make tumor tissues highly adaptable and resilient, making their treatment particularly challenging.

1.3. Chemotherapeutic strategies for cancer

In recent decades, significant progress has been made toward more effective cancer treatment methods, ranging from surgery and radiotherapy to immunotherapy and gene therapy. Nevertheless, the most widely used treatment for various types of malignancies remains chemotherapy [18], employed either as monotherapy or in combination with other therapeutic strategies. Chemotherapeutic strategies rely on the use of specific cytotoxic drugs that target different essential phases of the cell cycle, thereby interfering with cell division and proliferation and inducing apoptosis [19, 20].

Chemotherapy drugs can be classified based on their mechanism of action. For instance, topoisomerase inhibitors, such as doxorubicin and irinotecan, target topoisomerase enzymes, which are crucial for maintaining the 3D structure of DNA during replication. By inhibiting these enzymes, these drugs induce irreversible DNA damage, thus inducing cell apoptosis [18, 19]. Another drug class includes antimetabolites, such as 5-fluorouracil (5-FU) and methotrexate, which interfere with DNA and RNA synthesis, thereby inhibiting the proliferation of target cells. These agents are structural analogs of naturally occurring metabolites involved in polynucleotide synthesis, and exert their function by either replacing these metabolites or competitively inhibiting key enzymes during replication [19]. Although widely used for treating gastrointestinal and breast cancers, these drugs present significant limitations, particularly in terms of toxicity toward normal cells, leading to side effects such as damage to bone marrow and gastrointestinal tissues [21, 22]. Another key family of chemotherapeutic drugs includes mitotic spindle inhibitors, such as taxanes (paclitaxel and docetaxel) and vinca alkaloids (vinblastine). These drugs act by blocking mitotic spindle formation, leading to cell division arrest during mitosis. Specifically, paclitaxel acts by binding microtubule proteins, stabilizing their structure and

preventing the dynamic changes required for cell division, which ultimately induces cell death [18, 22]. Finally, the last category includes alkylating agents and platinum-based agents, such as cisplatin and carboplatin, which induce programmed cell death in target cells. These agents are widely used in treating various cancers due to their efficacy in damaging DNA and impairing cell replication [19].

1.3.1. Cisplatin: Mechanism of action

Cisplatin is a widely used chemotherapeutic drug for treating various types of malignancies, including lungs, bladder, ovarian, testicular cancers, and triple-negative breast cancer. As a drug belonging to the family of alkylating agents, its efficacy lies in its ability to directly bind to the DNA of target cells, forming complexes that disrupt the DNA structure, thereby impairing replication and transcription processes [23, 24].

Cisplatin was first discovered and studied in the cellular context by Barnet Rosenberg and his team around 1965. They observed that planar complexes containing Pt^{2+} ions in the cis configuration were particularly effective at arresting tumor models both in 2D *in vitro* and *in vivo* rat models [25]. Chemically known as cis-$[PtCl_2(NH_3)_2]$, cisplatin enters the bloodstream and diffuses into cells through mechanisms that are still not entirely understood. The most plausible hypothesis is simple passive diffusion through the hydrophobic lipid bilayer, due to its neutral charge [26]. Once inside the cell, it undergoes hydrolysis reactions, resulting in the removal of chloride ligands, which activates the drug. This highly reactive form of the molecule binds nucleophilic groups on the DNA strand [24]. The most favored reaction is the formation of covalent bonds with purine bases (guanine and adenine), leading to intra-strand (between nucleotides within the same DNA strand) or inter-strand adducts (between two different strands). The latter generally accounts for 90% of the alterations induced by cisplatin and causes a distortion in the DNA double helix, preventing its unwinding required for replication and transcription [23, 24]. This can trigger DNA damage response mechanisms, such as the p53 pathway, potentially leading to programmed cell death [27]. From a clinical perspective, this chemotherapeutic agent has shown the greatest efficacy with solid tumors characterized by defects in DNA repair mechanisms, such as certain types of breast cancer with specific mutations [27].

1.3.2. TNBC chemotherapy strategies

The characteristics of TNBC significantly limit potential therapeutic strategies, with chemotherapy remaining the primary approach. Among the most commonly used chemotherapeutic agents are taxanes, such as paclitaxel and docetaxel (from the mitotic spindle

inhibitor family), anthracyclines such as doxorubicin and epirubicin (topoisomerase inhibitors), and platinum-based drugs, including carboplatin and cisplatin. This last class of drugs has shown notable efficacy in TNBC patients with BRCA1 and BRCA2 mutations. These mutations impair DNA repair mechanisms following induced damage, increasing the sensitivity of the target malignancy to this class of drugs [24, 28]. Over time, combination therapies have been developed to enhance treatment efficacy. One example is the combined use of platinum-based agents with PARP (Poly ADP-ribose Polymerase) inhibitors. These further disrupt DNA repair processes in tumor cells, amplifying the drug's basic effect and leading to higher rates of cell death [29]. Additionally, other combination strategies involve immunotherapies, using immune checkpoint inhibitors (ICIs) which boost the body's immune response against tumor cells, offering a promising avenue for treating metastatic TNBC [30]. Ultimately, in the case of cisplatin, new drug delivery strategies have been developed to enhance its uptake and biodistribution. One promising approach is the use of nanocarriers, such as liposomes, which have demonstrated improved selective targeting of tumor cells. Liposomal delivery enhances cisplatin's bioavailability while reducing its systemic side effects by allowing for more controlled and localized release of the drug [22].

1.3.3. Challenges in treating TNBC with chemotherapy

Despite significant advances, chemotherapy remains limited by several key challenges, including drug resistance, systemic toxicity, and tumor heterogeneity, which often undermine long-term treatment effectiveness. Among these, drug resistance is a common issue in triple-negative breast cancer (TNBC) and other malignancies, manifesting either as acquired or intrinsic resistance [31]. One major mechanism of drug resistance involves the enhancement of DNA repair capabilities by neoplastic cells. They may activate repair pathways that correct the damage caused by certain chemotherapeutic drugs. In the specific case of cisplatin, resistant tumor cells are more effective at repairing cisplatin-induced DNA adducts or, equivalently, tolerating mismatches present in the damaged DNA strand. This resistance is facilitated by a specific class of DNA polymerases involved in translesion synthesis, allowing the cells to bypass and tolerate DNA lesions without triggering cell death [31]. Another important factor contributing to drug resistance is the reduced accumulation of chemotherapeutic agents at the intracellular level. In this case, resistance can be mediated by a decreased amount of drug intake, increased efflux, or inactivation of the agent itself. The ability of a chemotherapeutic agent to enter and accumulate within target cells is influenced by multiple factors, and is largely dependent on cellular transport systems. The upregulation or downregulation of specific

membrane transporters can be crucial to the effectiveness of chemotherapy. Several studies have demonstrated the association between so-called multidrug resistance (MDR) and certain relatively non-selective transporter proteins from the ATP-binding cassette (ABC) family, such as P-glycoprotein, which function as pumps expelling chemotherapy drugs from cells and preventing the drugs from reaching effective intracellular concentrations [24, 31]. In the specific case of cisplatin, a strong correlation has been observed between drug effectiveness and certain transporters. Studies have revealed a positive correlation between intracellular uptake of the drug and the presence of active copper transporters, such as CTR1 and CTR2, as well as organic cation transporters like OCT. Conversely, ATP7A and ATP7B, two copper-exporting transporters, can reduce the drug's efficacy by promoting its efflux, thereby contributing to resistance [24].

Another crucial factor contributing to MDR is the process of drug inactivation or detoxification within the cell. At the intracellular level, specific molecules may bind to the chemotherapeutic drug neutralizing it, thereby preventing its cytotoxic effect. For cisplatin, interaction with nucleophilic cytoplasmic proteins, such as glutathione (GSH), methionine, metallothionein, and other cysteine-rich proteins can significantly reduce its effectiveness [23, 24, 31]. Several studies, both *in vitro* and *in vivo*, have highlighted a correlation between high levels of glutathione and resistance to cisplatin in tumors, although no clinical significance has been yet demonstrated [32, 33]. A major limiting factor in chemotherapy is the toxicity induced in healthy tissues. Chemotherapeutic agents while aiming to destroy cancer cells, are not always highly specific and can also damage normal proliferating cells. his lack of selectivity often leads to cytotoxic effects in tissues with high turnover rates [18]. A well-known example is myelotoxicity, or bone marrow suppression, which impairs the production of red blood cells, white blood cells, and platelets, leading to conditions such as anemia, leukopenia, fatigue, and increased susceptibility to infections [28]. Damage other rapidly dividing tissues, such as the gastrointestinal system, can also occur, causing inflammation, ulcers, and nausea. Furthermore, cardiotoxicity and peripheral neurotoxicity are common side effects associated with certain chemotherapeutic drugs, including taxanes and platinum-based agents [18, 28]. In particular, cisplatin is frequently associated with side effects such as myelotoxicity, nephrotoxicity (kidney damage), and ototoxicity (hearing loss). These effects may limit therapy to lower drug doses, thereby reducing treatment efficacy [23, 28, 34] Overall, the issues associated with current therapies highlight the need for alternative treatments that enhance efficacy and reduce side effects.

1.4. Alternative treatments

1.4.1. Influence of diet and nutrient availability on tumor progression

As previously noted, tumors are characterized by a heterogeneous, dynamic, and altered metabolism that is crucial for fulfilling intrinsic biosynthetic, bioenergetic, and signaling demands of rapidly proliferating cells [35]. Tumor metabolism is shaped by multiple factors, including genetic factors, cell population, anatomical location, structural properties, and environmental factors [36–38]. Among these, environmental factors specifically modulate nutrient availability, which plays a dominant role in defining cancer cell metabolism [39, 40]. The availability of nutrients to tumor cells is largely determined by metabolites produced by neighboring cells and the nutrients circulating within the endothelial vessels that supply the tumor [35]. These metabolites are also strongly influenced by dietary intake, which explains why dietary habits can significantly impact on the type and concentration of metabolites available to tumor cells [41].

Various studies have highlighted the effects of different diets on overall health and, more specifically, on neoplasia progression and development. For instance, the Western diet, characterized by high levels of processed foods, fats, and sugars, is associated with higher incidences of obesity and coronary diseases. Furthermore, in the United States, it has been observed that excessive body weight is a risk factor for cancer across at least 13 different anatomical sites, with obesity-related cancer mortality accounting for 14-20% of all cancer deaths [42]. Conversely, the Mediterranean diet, which emphasizes fruits, vegetables, whole grains, and healthy fats, appears to be associated with longer life expectancy and potentially lower cancer risk [35].

In recent years, an increasing number of studies in the scientific community have sought to better understand if and how targeted diets could potentially exploit the unique metabolic characteristics and vulnerabilities of tumors to fight cancer more effectively. The core concept is to use specific diets to strategically manage nutrient availability, thereby sensitizing target tumors and improving the efficacy and response to conventional cancer treatments [42–44]. Several mostly preclinical studies suggest that dietary restrictions may influence various stages of tumor initiation, progression, and metastasis [45], and when combined with chemotherapy, they may alleviate the adverse effects of these therapies and enhance their effectiveness [46].

However, it should be noted that not all tumors are share the same metabolic profile, and therefore, not all tumor types may be equally amenable to targeting via diet. Moreover, a

single, universal strategic diet cannot be applied, but diet must be tailored to the specific metabolic needs and vulnerabilities of individual tumors [42].

1.4.2. Diet strategies and synergy with chemotherapy

In recent decades, various types of diets have been designed and studied, optimized according to specific dietary regimens and/or nutritional restrictions. These diets focus on defined metabolic objectives to achieve an overall positive physiological response in both healthy and pathological subjects. Below, some of the most studied diets in the oncological context are analyzed.

Ketogenic diet. The ketogenic diet (KD) is characterized by a high-fat intake (90%), moderate protein intake (8%), and a drastic reduction in carbohydrates (2%) [42]. Physiologically, it induces a metabolic state of ketosis in subjects, leading to high circulating levels of ketone bodies that are used as the primary energy source in place of glucose [35].

At the physiological level, it reduces plasma glucose levels while increasing ketone bodies, such as β-hydroxybutyrate and acetoacetate. At the cellular metabolic level, these ketone bodies bypass cytoplasmic glycolysis and enter the tricarboxylic acid (TCA) cycle directly as acetyl-CoA, thereby supporting healthy cells, which typically utilize non-glycolytic energy sources unlike many cancer cells that rely heavily on glucose (Warburg effect) [38]. Additionally, at the tissue level, KD induces a reduction in stromal inflammation and decreases factors such as IGF-1, which are typically known to promote tumor growth [47].

For these reasons, the ketogenic diet has been studied in oncology to potentially control tumor growth and progression [45]. Its effects have been evaluated with or without other anti-tumor therapies, including chemotherapy. Preclinical studies have shown a positive synergistic effect between chemotherapy and KD, leading to increased efficacy. In murine models of pancreatic cancer, tumor cells exhibited increased sensitivity to cytotoxic therapy, tripling the survival benefits of conventional chemotherapy (gemcitabine, nab-paclitaxel, cisplatin) [48]. Other studies in murine breast cancer models demonstrated that combining this diet with other therapies could potentially have positive effects, as observed by reduced tumor growth in situ, inhibition of metastasis, and a delay in the increase of circulating tumor cells (CTCs) [49].

Clinically, the effectiveness of this diet is also being experimentally tested, though progress is gradual. However, the limited number of patients adhering to the therapies and challenges in ensuring compliance with dietary regimens have led to inconsistent and often non-significant results. Some clinical trials have observed beneficial effects of KD during cancer

therapy, albeit with few participants and experimental setups that are not always clear and lack rigorous controls [50, 51]. Studies in patients with advanced-stage breast cancer with metastasis have shown higher survival rates in subjects treated with neoadjuvant therapy compared to controls, with cases of complete metastasis remission. A reduction in the expression of a tumor marker associated with aerobic glycolysis (transketolase-like 1, TKTL1) was also observed in patients strictly adhering to KD supported by medium-chain triglycerides (MCTs), which provide critical support in terms of immediate energy, cognitive function, and maintenance of ketosis [52, 53].

Overall, regardless of survival outcomes, patient adherence to KD during anti-tumor therapy can potentially induce benefits, such as better maintenance of skeletal muscle mass and an overall more favorable physical condition.

Caloric restriction. Caloric restriction (CR) is a diet that involves a reduced caloric intake (around 15-40%) without causing malnutrition, aiming to positively influence metabolic functions and improve overall health [42]. Various studies have indicated that CR may yield benefits ranging from a possible slowing of aging and delay of age-related conditions [54], improvements in several biomarkers, reduction of general inflammatory states, and even potential oncological benefits [55–57].

The benefits of CR appear to be associated with several biological effects, including lowered circulating levels of various hormones, growth factors, and cytokines. One key target is insulin-like growth factor 1 (IGF-1), which plays a critical role in pathways such as RAS/MPK and PI3K/AKT/mTOR, typically dysregulated in tumors and involved in promoting their growth [43, 58].

CR-induced effects in murine tumor models also include the activation of autophagy, a "self-digestion" process that allows cells to eliminate damaged components and survive under metabolic stress conditions. Autophagy can play a dual role in cancer: while it can reduce oncogenic potential by clearing damaged cellular components, it may also support the survival of certain cancer cells, contributing to treatment resistance [59]. This highlights the need to carefully consider the context and tumor type when evaluating the impact of CR on cancer treatment.

Other *in vivo* animal studies have also investigated the effects of this diet in combination with chemotherapy. Preclinical studies have shown that CR increases the sensitivity of cancer cells to cytotoxic therapy, enhancing treatment efficacy [43, 45]. Specifically, in cancers characterized by cells with heightened glycolytic metabolism, such as breast and cervical cancers, reducing glucose intake (the primary energy source) has led to decreased

proliferation and invasive capacity [60]. In murine melanoma models, caloric restriction has shown synergistic effects in enhancing therapeutic response by increasing cancer cell sensitivity to cisplatin, reducing resistance, and promoting apoptosis [59]. Other preclinical studies on breast cancer have demonstrated that CR, in combination with other therapies, leads to reduced tumor progression and metastasis inhibition, delaying the increase of circulating tumor cells (CTCs) [49].

These findings suggest potential benefits in integrating CR with standard therapies for the treatment of triple-negative breast cancer [42]. However, further clinical studies are necessary to validate the effectiveness of this strategy in different oncological contexts.

Fasting. Fasting-based diets, commonly known as "fasting," encompass various strategies such as intermittent fasting, the fasting-mimicking diet (FMD), and others. These approaches have been studied as potential adjuvants to oncological therapy due to observed metabolic and immunological benefits. Intermittent fasting (IF) involves alternating between fasting and feeding periods, typically organized in cycles of 16-24 hours of fasting followed by short eating windows [61]. The FMD, on the other hand, aims to mimic the physiological effects of prolonged fasting while maintaining a minimal nutrient intake (200-1100 kcal per day) [62]. Both approaches seek to modify the tumor microenvironment and reduce the availability of nutrients that may promote tumor growth [42].

Fasting induces significant changes at both physiological and cellular levels. Systemically, it reduces blood glucose, insulin, and insulin-like growth factor 1 (IGF-1) levels. In cancer cells, this inhibits anabolic processes and promotes increased sensitivity to chemotherapy. Cancer cells also undergo metabolic modulation, reducing glycolysis and promoting apoptosis [35]. FMD, in particular, has shown promising results in preclinical studies. In murine models, this diet has been associated with modulation of the antitumor immune system, reducing regulatory T cells (Tregs) and increasing cytotoxic T cell (CD8+) infiltration, thereby promoting a stronger immune response against the tumor [35, 63, 64]. Another study demonstrated the synergistic effects of FMD with anti-angiogenic agents such as apatinib. A reduction in hypoxic tumor-associated macrophage (TAM) infiltration was observed, along with decreased tumor growth and restricted lung metastasis [64]. This illustrates fasting's ability to significantly impact the tumor microenvironment by reducing pro-tumoral cell populations and modulating the tumor's metabolic responses.

Additional studies on murine models of triple-negative breast cancer (TNBC) have highlighted fasting's potential positive effects on more aggressive tumors. A significant reduction in cancer stem cells (CSCs), which play a crucial role in treatment resistance and cancer recurrence, was observed due to the downregulation of glucose-dependent PKA

signaling. In differentiated cancer cells, the activation of "escape from fasting" pathways (including PI3K/AKT, mTOR, and CDK4/6) was noted, suggesting the potential for treating the tumor in combination with drugs that block these pathways [65].

The beneficial effects of fasting have also been documented in clinical settings. In a cohort study of patients with non-metastatic breast cancer, high blood glucose levels were associated with poorer prognosis, suggesting that glycemic control may play an important role in improving clinical outcomes [66]. In addition, FMD has shown potential for protecting patients from the cytotoxic side effects of chemotherapy. Clinical studies have reported that chemotherapy, when combined with FMD or IF, resulted in an enhanced therapeutic response and reduced DNA damage in healthy cells, such as immune cells (T lymphocytes) [67], while also improving patients' quality of life by reducing side effects like fatigue and nausea [61].

Other specific clinical studies on TNBC patients appear to confirm the effectiveness of combining chemotherapy and fasting to treat cancer and improve the overall condition of patients undergoing treatment. In advanced TNBC patients treated with a combined fasting and chemotherapy regimen with carboplatin and gemcitabine, a significant improvement in overall survival (OS) was observed, along with enhanced pathological response and a reduction in cancer stem cell markers. Fasting also positively influenced immune response modulation, increasing cytotoxic T cells and reducing regulatory T cells [68].

However, it should be noted that some preclinical studies have shown that fasting may not always be effective in cancer prevention and treatment, indicating the need for further research to determine the optimal conditions for applying these dietary strategies [45]. Moreover, despite promising results, the clinical translation of fasting strategies still faces numerous challenges. Significant obstacles include variability in study protocols and difficulties in patient adherence to dietary restrictions. Additionally, preclinical models, often animal-based, do not always accurately reflect the complexity of the human tumor microenvironment, limiting the translatability of the results to humans. Therefore, it is essential to develop more advanced preclinical models, such as organ-on-chip platforms, that can more accurately represent the interactions between cancer cells and their microenvironment.

1.5. Tumor models

1.5.1. Animal models, *in vitro* and *ex vivo* models

Tumor models are essential components of oncology research, providing critical insights into tumor biology, facilitating drug screening, and enabling therapeutic development. Due to the complex nature of tumors, a combination of model systems, including animal (*in vivo*), *ex vivo*, and *in vitro* models, is necessary, each offering distinct advantages and limitations for studying various aspects of cancer biology and treatment response.

In vivo models, typically involving laboratory animals such as mice, rats, and zebrafish, are fundamental for investigating tumor initiation, progression, and therapeutic efficacy within a living organism. These models facilitate the study of systemic effects including immune responses, as they capture the dynamic interaction between the tumor and the host environment. However, *in vivo* models are associated with several significant limitations, including high costs, low reproducibility, and ethical concerns [69]. Moreover, inherent biological differences between animal models and humans often result in limited translatability of findings, with fewer than 8% of treatments that demonstrate efficacy in animal models ultimately proving effective in human clinical trials [70]. Despite these limitations, *in vivo* models remain often essential for assessing drug toxicity, pharmacokinetics, and immune-related effects [71].

In vitro models address some of the challenges associated with *in vivo* studies by allowing the controlled investigation of biological samples outside of the living organism (Hickman et al., 2014). These models include two-dimensional (2D) and three-dimensional (3D) cell culture systems. While 2D cultures are cost-effective and suitable for high-throughput screening, they fail to capture the complexity of the tumor microenvironment. In contrast, 3D cultures more accurately replicate tumor architecture, including cell-cell and cell-matrix interactions, as well as gradients of oxygen, nutrients, and signaling molecules, thereby improving the predictive accuracy of drug responses [72]. Recent innovations, such as the integration of 3D cultures with bioreactors, have further enhanced their physiological relevance, enabling dynamic flow conditions that better simulate the *in vivo* environment.

Ex vivo models, involve the extraction of tissues or organs from a living organism for study under controlled conditions that preserve much of the native tissue architecture and functionality [72]. In fact, these models maintain cellular heterogeneity and tumor-stroma interactions allowing researchers to explore local tumor dynamics, including microenvironmental influences that are difficult to replicate *in vitro*. However, *ex vivo* models come

with their own limitations. Tissue samples are variable, with differences stemming from factors like donor age, sex, and health status. Additionally, the viability of extracted tissues is often limited, restricting the utility of *ex vivo* models to short-term studies.

While both *in vitro* and *ex vivo* models involve examining biological samples in controlled environments, they differ substantially in complexity and applicability. *In vitro* models are highly scalable and suitable for mechanistic studies and drug screening, but they often lack the intricate architecture and microenvironment present in native tissues. *Ex vivo* models, on the other hand, retain the complexity of native tissue, including cell diversity and structural integrity, making them valuable for studying tumor-stroma interactions and local microenvironmental effects. *in vivo* models are frequently considered the gold standard for evaluating drug efficacy and safety, given their ability to recapitulate systemic physiological responses. However, their use is constrained by ethical concerns, high costs, and low predictive accuracy for human outcomes [70].

1.5.2. Importance of 3D environment and dynamic culture condition

Three-dimensional *in vitro* models are emerging as a preferred choice in preclinical research due to their capacity to closely mimic tumor architecture while providing scalability and ethical advantages [72]. Three-dimensional (3D) tumor models represent a major advancement over traditional two-dimensional (2D) cultures, providing a more physiologically relevant replication of the tumor microenvironment. Unlike 2D models, where cells grow as flat monolayers on rigid surfaces, 3D models enable cells to develop in a spatially organized architecture that closely mimics *in vivo* conditions. This arrangement allows for intricate cell–cell and cell–extracellular matrix (ECM) interactions, as well as the establishment of biochemical and nutrient gradients, thereby offering a more accurate representation of tumor biology [73]. While 2D cultures are widely used for high-throughput screening due to their simplicity, they have significant limitations in replicating the tumor microenvironment. The lack of three-dimensional architecture prevents 2D models from accurately mimicking the spatial organization and gradients found in real tumors, leading to altered cellular behavior and reduced predictive value for preclinical studies [74]. In contrast, 3D cultures, such as spheroids, better replicate tumor features like proliferation gradients (e.g., proliferative, quiescent, and necrotic regions) and chemical heterogeneity [75]. These qualities make 3D models more effective for evaluating drug efficacy, yielding results that better predict *in vivo* outcomes compared to 2D systems. The main features of the two models are outlined in Figure 1.2.

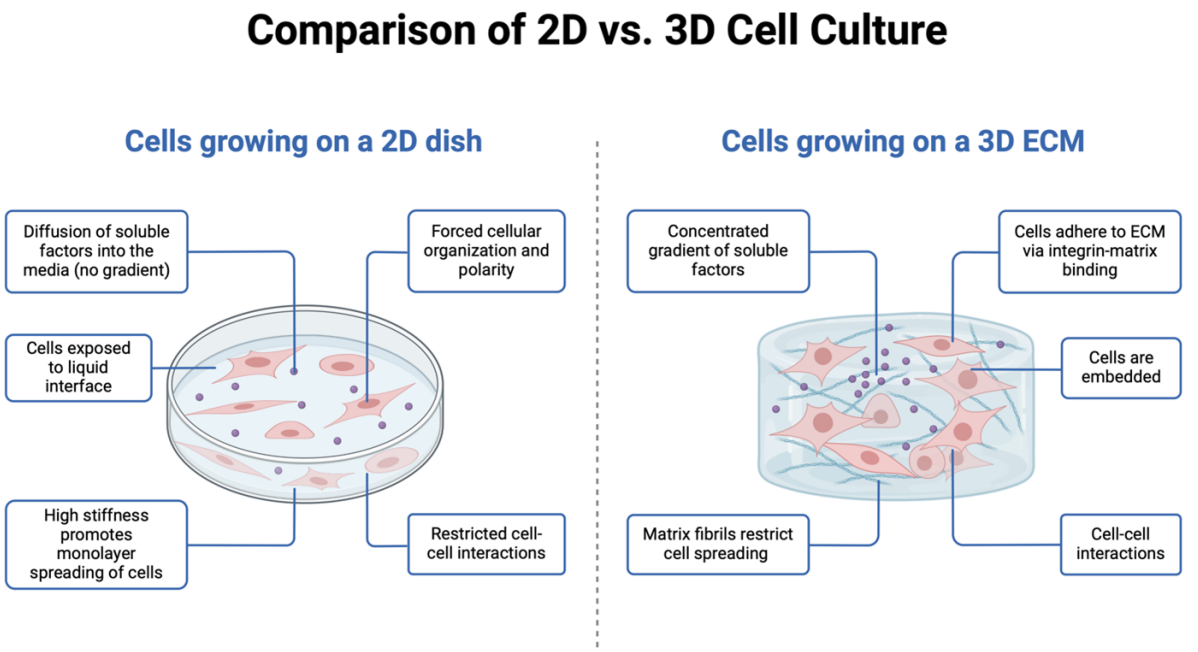

Figure 1.2: Comparison between 2D and 3D cell cultures. In 2D cultures, cells grow on a flat surface, exposed to a liquid interface, with limited cell-cell interactions and no gradient of soluble factors. In contrast, 3D cultures allow cells to adhere to the extracellular matrix (ECM), where they are embedded, promoting more complex cell-cell interactions and a gradient of soluble factors, creating a more realistic representation of tissue architecture. Edited on Biorender.com

Recent advancements in 3D model development have integrated key elements of the tumor microenvironment, such as stromal cells, immune components, and ECM, thereby improving the biomimetic properties of these models [76]. Moreover, the incorporation of microfluidic devices and bioreactors has further enhanced the physiological relevance of these systems. Dynamic culture conditions, which simulate fluid flow akin to blood circulation, recreate the mechanical stimuli necessary for cell differentiation, nutrient distribution, and waste removal, more effectively mimicking *in vivo* conditions compared to static cultures [77].

Dynamic culture systems offer several critical advantages over static conditions. In dynamic environments, cells are exposed to continuous fluid flow, ensuring a consistent supply of nutrients and oxygen while efficiently removing metabolic waste. This enhanced culture environment not only efficiently supports cell viability and proliferation but also induces behaviors that are more representative of *in vivo* conditions, such as increased angiogenic potential and reduced apoptotic signaling [77]. Furthermore, bioreactors used alongside dynamic 3D cultures allow for precise control over environmental parameters, such as pH, oxygen levels, and shear stress, thereby creating a model that more accurately reflects the tumor microenvironment [72].

1.5.3. Organ-on-chip technology: advantages and applications

Recent advancements in biomedical engineering have led to the development of new advanced and transformative *in vitro* models: Organ-on-chips (OoC). These technologies better emulate the physiological functions of human organs by integrating fluidics, advanced materials, and cell biology. The systems consist of fluidic channels and biological components (such as cells, tissue, biopsy) housed in environments that range from micro- to macro-scale, effectively mimicking *in vivo* conditions. OoC platforms, also known as Microphysiological Systems (MPSs), enable precise control over biochemical and mechanical stimuli, such as fluid flow, shear stress, and nutrient gradients-factors critical for replicating the human tissue microenvironment [78]. Therefore, the fluidic network along with the possibility to establish a continuous flow of culture medium, may simulate blood circulation and generate dynamic conditions that closely resample those *in vivo*. Unlike traditional static cell culture models, OoC technology replicates tissue-level functionality, including organ-specific signaling, mechanical forces, and human tissue interactions. This makes it a powerful tool for investigating complex physiological processes, disease mechanisms, and drug responses, and it is particularly beneficial for pharmacokinetics, toxicity assessments, and personalized medicine, ultimately improving preclinical testing outcomes [78, 79].

As the field evolved, there was a shift towards designing microfluidic devices that were less miniaturized but more intricate, with the goal of better replicating physiological conditions. This shift aimed to create clinically relevant models of human tissues and organs cultured under dynamic fluid conditions. Initially, many microfluidic devices were static or relied on gravity forces to induce a dynamic flow through chip tilting. The gravity-driven method is based on a system of communicating vessels, where the microfluidic channel is connected to two reservoirs filled with liquid at different heights [80, 81]. In these systems, flow is induced by the hydrostatic pressure difference of fluid levels in connected reservoirs [82]. While avoiding the need of external pumps and tubing, this method carries several limitations, including poor control of the dynamic environment and the inability to establish a unidirectional flow [83]. More recently, OoCs equipped with external pumps for fluidic flow induction have been developed. These devices enable the culture of cells under vasculature-like perfusion in a precisely controllable microenvironment, resulting in physiologically-relevant *in vitro* models of human tissues and organs. The introduction of peristaltic pumps has been particularly transformative, as they facilitate circulatory, unidirectional fluid flow, which is crucial for the administration of nutrients and timely waste discharge. Constant flow in organ-on-chip systems ensures a steady supply of nutrients and oxygen to the cells while efficiently removing waste products. This helps maintain

cell viability and function over extended periods, which is particularly important for long-term studies and accurate modelling of disease progression and treatment responses. This dynamic environment closely mimics physiological conditions, generating fluid shear stress that induces organ polarity [84]. At the microscale level, fluid in these systems primarily acts as laminar flow, allowing individual streams of fluid to flow separately without a physical barrier between them. This creates a stable gradient of biochemical molecules, which physiologically regulates several biological phenomena, including angiogenesis, invasion, and cell migration. By replicating these complex *in vivo* conditions, modern OOC devices provide more accurate and reliable models for studying human biology and disease mechanisms [85]. *In vivo*, cells are exposed to various mechanical forces, including shear stress from blood flow. Flow in organ-on-chip devices replicates these forces, influencing cell behaviour, differentiation, and function. This is vital for studying how cancer cells metastasize and how immune cells migrate and infiltrate tumors.

In cancer research, cancer-on-chip models have significantly advanced the study of tumor biology under controlled, physiologically relevant conditions. Cancer-on-a-chip represents a ground-breaking advancement in the field of OoC technology, specifically tailored to emulate the intricate characteristics of cancerous tissues *in vitro* for both accelerating the knowledge of molecular mechanisms behind human cancer progression and for advancing the testing of effective therapeutics. Moreover, they offer a promising avenue for advancing cancer research and personalized medicine.

One of the key innovations of cancer-on-chip technology is its ability to integrate OoCs with three-dimensional (3D) cancer models, thereby mimicking the complex spatial and temporal behaviour of tumours. This integration involves the incorporation of different cell types, such as cancer cells, stromal cells, and blood vessel cells, allowing researchers to replicate the dynamic interplay between these various cell types. Such a setup facilitates a more accurate representation of tumour growth, invasion, and response to therapeutics. In some cases, such cells are embedded in a tumour extracellular matrix resembling that of the tumour microenvironment (TME), which modelling *in vitro* enables the study of key aspects such as angiogenesis, metastasis progression, and drug resistance. Replicating the complex TME is indeed crucial for the testing and development of novel therapeutic approaches. Additionally, the possibility to integrate the platform with a control and measurement system, enable real-time monitoring of tumor behavior during therapeutic intervention, providing valuable data on drug efficacy and resistance [86]. Moreover, by simulating blood flow, mechanical forces, and ECM interactions, these devices allow detailed observation of cancer cell migration and metastasis [87].

Overall, organ-on-chips offer unparalleled advantages in replicating the physiological com-

plexity of human organs, providing a robust alternative to traditional models for disease modeling, drug screening, and personalized medicine. Particularly in fields such as oncology, these technologies hold great promises for enhancing anti-tumor drug development, testing new therapy approaches, and advancing personalized cancer treatment strategies [86]. Furthermore, cancer-on-chip platforms enable the investigation of patient-specific tumor responses, paving the way for advancements in personalized medicine. By using cells derived from individual patients, these devices can be used to test the efficacy and toxicity of potential treatments on a patient-by-patient basis. This approach holds the potential to tailor treatments to the unique characteristics of each patient's cancer, improving therapeutic outcomes and minimizing adverse effects. Within the cancer on chips, the presence of flow allows for more realistic drug delivery and distribution within the tissue model, leading to more reliable data on drug efficacy and toxicity. This enhances the predictive power of preclinical testing and helps in identifying potential therapeutic candidates earlier in the development process. Moreover, flow conditions facilitate the recruitment and movement of immune cells within the chip, closely mimicking the immune response in the human body. This is particularly important for immuno-oncology studies, where understanding the interaction between immune cells and cancer cells is critical for developing effective therapies. In particular, recruitment of human immune cells into the tumor tissue is an essential step that shapes the immune microenvironment and defines the ability of a tumor to respond or not to immune targeting strategies, finally leading to a positive or negative outcome.

1.6. Rationale of the study

Triple-negative breast cancer (TNBC) is a highly aggressive subtype of breast cancer characterized by its poor prognosis and limited treatment options. Despite advancements in cancer therapies, the efficacy of conventional treatments like cisplatin remains suboptimal due to the metabolic heterogeneity of tumors. In this context, evaluating how glucose levels influence the response to cisplatin-based therapy is critical, as tumor metabolism plays a key role in treatment resistance and efficacy.

1.6.1. Objective of using simplified 3D model Of TNBC

The objective of this study is to develop a simplified three-dimensional (3D) model of TNBC using alginate hydrogel and a single cell line to better simulate the tumor microenvironment. The 3D model provides a more accurate representation of the physiological conditions of tumors, as it allows for the maintenance of cell-to-cell and cell-matrix in-

teractions, crucial factors in cancer progression and treatment responses. The use of a simplified model with alginate hydrogel ensures a controlled and reproducible system for studying glucose metabolism in TNBC cells.

Alginate is a naturally occurring polysaccharide derived from brown seaweed, commonly used in 3D cell culture models due to its biocompatibility, versatility, and ability to form gels under mild conditions. However, while the simplicity of an alginate-based system is an asset for certain applications, it also presents significant limitations. Notably, it does not fully replicate the complex tumor microenvironment, which includes the presence of stromal cells, immune cells, and complex ECM components that are critical for tumor progression and therapeutic responses. Despite these limitations, the simplicity of an alginate-based model remains a crucial advantage, particularly when the goal is to isolate and study specific factors, such as glucose levels or chemotherapy effects, in a controlled and reproducible manner. The design of relatively simple yet effective 3D tumor models allowed to conduct a more focused study on effects of glucose on cisplatin-based treatments in triple-negative breast cancer (TNBC), without the confounding complexity of more advanced systems.

1.6.2. Hypothesis: effect of glucose levels and cisplatin treatment on TNBC behavior

The aim of this study is to evaluate the effects of varying glucose levels on the response of triple-negative breast cancer (TNBC) cells to cisplatin-based chemotherapy. This focus is crucial because glucose metabolism is frequently dysregulated in cancer cells (Warburg effect), where cancer cells preferentially utilize glycolysis for energy production, even in the presence of oxygen. This metabolic shift has profound implications for how cancer cells respond to treatment, including chemotherapy. Understanding the link between glucose metabolism and chemotherapy response in TNBC could pave the way for more personalized and effective treatment strategies. By investigating the effects of varying glucose levels on cisplatin-based treatment, this study seeks to uncover novel ways to enhance the efficacy of chemotherapy in TNBC, potentially improving outcomes for patients with this challenging and aggressive cancer.

1.6.3. Simulating *in vivo* condition: MIVO® organ-on-chip technology

To simulate *in vivo* conditions more closely, the study incorporates MIVO® (Microfluidic In Vitro Organ) organ-on-chip technology, which integrates fluidic flow dynamics and can-

cer cell culture in a microenvironment resembling the human tumor tissue. By mimicking the complex *in vivo* conditions, this model will provide valuable data on tumor metabolic behavior and its interaction with cisplatin therapy, helping to bridge the gap between preclinical findings and clinical applications. The introduction of fluid-dynamic stimuli to the 3D cells culture indeed remarkably improves the relevance of *in vitro* models, leading to a deeper investigation of cancer cells infiltration, cancer-immune cells cross-talk and novel anti-cancer testing therapies. In this context, the commercially-available MIVO® organ-on-chip is composed by an optically transparent cell culture chamber compatible with the 24-well plate's size inserts, where clinically relevant size cancer tissues are cultured under physiological flow conditions.

2 | Materials and methods

2.1. Cell cultures

MDA-MB-231. Commercially available human MDA-MB-231 cells were used. MDA-MB-231 is an adherent cell line derived from pleural effusion of primary triple-negative breast adenocarcinoma. Cells were thawed in a 37°C water bath (PolyScience, Niles, Illinois, USA), then seeded into T75 cell culture flasks (Euroclone S.p.A., Milan, Italy) and cultured in DMEM high glucose (Gibco™, Waltham, Massachusetts, USA), supplemented with 10% Fetal Bovine Serum (FBS, Euroclone S.p.A) and 1% Penicillin-Streptomycin mixture (P/S) (Euroclone S.p.A.), hereafter referred to as complete MDA medium. Cells were maintained at 37°C and 5% CO_2 into the incubator Forma Series 3 Water Jacket (Thermo Fisher Scientific, Waltham, Massachusetts, USA). Culture media was refreshed every 2-3 days by removing the exhausted media, gently washing the flask with pre-warmed Dulbecco's Phosphate Buffered Saline (PBS) w/o calcium and w/o magnesium (Euroclone) and adding 8 mL of new fresh culture media. Cells were sub-cultured upon reaching confluence. For the sub-culturing procedure, after the removal of exhausted media, and a washing step with 5 mL of prewarmed PBS, 2 mL of Trypsin-EDTA 1X in PBS w/o Phenol Red, w/o Calcium, w/o Magnesium (Euroclone) were added to the flask and incubated for 8 minutes at 37°C. Cell detachment was monitored using an inverted microscope (Nikon Eclipse Ts2-FL, Nikon Europe B.V. Amstelveen, The Netherlands). Subsequently, 4 mL of pre-warmed complete culture medium were used to wash the flask and to deactivate trypsin enzymatic action. Cell suspension was transferred into a 15 mL tube (Eurcoclone S.p.A) and centrifuged (SL 8, Thermo Fisher Scientific, Waltham, Massachusetts, USA) at 300 G for 5 minutes. Supernatant was then removed, and cell pellet resuspended in 1 mL of medium. Cells were manually counted using a Neubauer chamber and reseeded at the density of 4.0-7.0 x 10^4 cells/cm^2 for cells expansion or used for the experiments described below.

HDFas. Normal human dermal fibroblasts (HDF) obtained from CELLnTEC Advanced Cell Systems (Sitem MedTech Hub (SMH), Bern, Switzerland) were thawed in a 37°C

water bath then seeded into T75 cell culture flask and cultured in DMEM High Glucose (Euroclone), supplemented with 10% FBS, 1% P/S, 2 mM L-Glutamine, henceforth called complete HDF medium. Culture media was replaced every 2-3 days. Once confluence was reached, cells were sub-cultured, by incubation with Trypsin-EDTA 1X, subsequent cell centrifugation at 300 G for 5 minutes and final counting. Cells were reseeded at the density of 4.0-7.0 x 10^4 cells/cm2 for cells expansion or used for the experiments described below.

2.2. 2D Model

For the realization of 2D models, a cellular suspension obtained as explained before was used. The suspension was diluted to obtain a final concentration of 15.000 cells/mL. The 2D model consisted in seeding 1 mL of the new cell suspension into a well of a Cellstar 24-well plate (Greiner Bio-One GmbH, Kremsmünster, Austria). Cells were maintained into the incubator at 37°C and 5% CO_2 for 24 hours after the seeding. Afterward the 24-well plates were subjected to removal of the culture medium and washed with a pre-warmed physiological solution 0.9% NaCl (Ecotainer®, B. Braun, Milan, Italy) with 5 mM $CaCl_2$. Subsequently the 24-well plates were filled with 1 mL of culture media specific for the study conditions.

2.3. 3D Model

Cell-laden 3D hydrogels were generated by mixing either MDA-MB-231 or HDFas cells with a 2% (w/v) Alginate solution (React4life S.p.A., Genoa, Italy), to recapitulate a 3D cancer model and a 3D healthy control, respectively. In detail, cells were resuspended in complete medium at the concentration of 1.5 x 10^6 cells/mL and then mixed with a solution of 2% (w/v) Alginate gel in physiological solution 0.9% NaCl (Ecotainer®, B. Braun, Milan, Italy), at 1:1 ratio, to obtain a final cell concentration of 7.5 x 10^5 cells/mL in 1% (w/v) Alginate gel. Obtained alginate-cell suspensions were dropped by using a 1 mL syringe, into a Petri dish previously filled with 0.5 M of $CaCl_2$ (Cross-linking solution), for physical crosslinking. Each gel was formed by using 20 µL of cells suspension, containing about 1.5 x 10^4 cells. After a few minutes of stabilization, cross-linking solution was removed and replaced with 3 mL of complete culture medium supplemented with 5 mM $CaCl_2$ (gel culture medium). Gels were cultured for 24 hours, then the 3D models were either cultured in static conditions or moved into the MIVO® organ-on-chip for dynamic culture.

2.4. Dynamic clultures

The emulation of *in vivo* dynamic physiological flow was achieved using the commercial organ-on-chip (OoC) device MIVO® Single Flow developed by React4life S.p.A. (Genoa, Italy). The procedure was performed in sterile conditions within a biological hood. Each MIVO® was covered with the specific lid and secured to the proper holder, before being connected to a pump tube via appropriate male-female luer-lock connections, to create a closed circuit. Cell culture medium was then injected into the basal circuit, through a three-way valve, by using a syringe with a needle. The basal chamber of the device and the circuit itself were filled with a volume of approximately 3.5 mL. The 3D cancer models were transferred into 24-well inserts with 8 µm pore size (Greiner Bio-One GmbH, Kremsmünster, Austria) previously filled with 250 µL of culture medium (2 hydrogels for each insert). One insert for each MIVO® Single Flow was then placed inside the device chamber. The circuit was finally connected to a peristaltic pump (RJ100, React4life) by using a dedicated cartridge fig. 2.1.

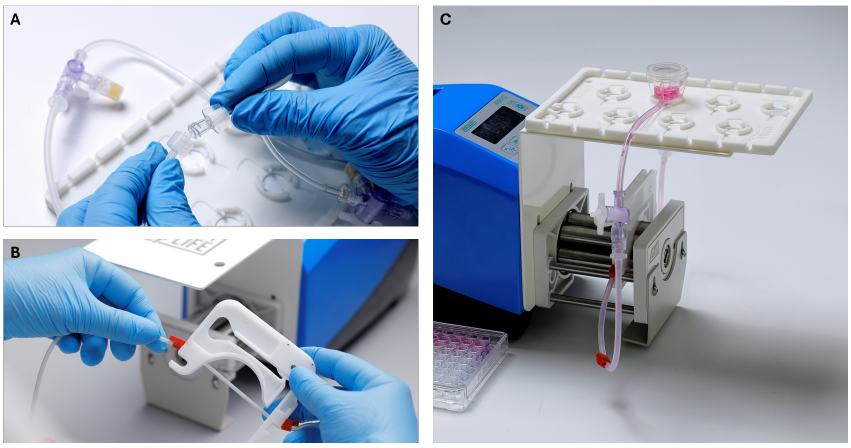

Figure 2.1: Device setup. (A) Luer-lock tube connectors. (B) Cartridge. (C) Complete system: one MIVO® single flow chamber, holder, tube, cartridge , and peristaltic pump.

The whole dynamic culture system was moved into the incubator at 37°C and 5% CO_2. To simulate a physiological flow, the pump was set to ensure a flow rate of 1 mL/min in the circuit.

2.5. Fasting simulation

The administration of different glucose-containing diets as an integrated approach for cancer treatment was simulated by using culture media containing different concentrations of glucose, and their effects on the viability of tumor *in vitro* models were evaluated.

Three different experimental groups were considered: No glucose, Low glucose, and High glucose as control. Glucose levels were recapitulated by using DMEM High glucose (4.5 g/L D-Glucose, 110 mg/L Sodium Pyruvate, L-Glutamine) DMEM Low glucose (1 g/L D-Glucose, 110 mg/L Sodium Pyruvate, L-Glutamine), or DMEM no glucose (0 g/L D-Glucose, 0 mg/L Sodium Pyruvate, L-Glutamine), as culture medium (Gibco™, Waltham, Massachusetts, USA). A preliminary experiment was conducted in a first optimization step, where the effect of different FBS concentrations on 2D cell culture, with different glucose levels, were investigated. MDA-MB-231 were seeded in 24-well plates (1.5 x 10^4 cells/well) and cultured in complete medium for 24h to allow proper attachment. Medium was removed and cells were treated with 1 mL of various glucose-containing culture media: DMEM High glucose (High G), DMEM Low glucose (Low G) or DMEM No glucose (No G), supplemented with 1% P/S and either 0%, 2%, 5% or 10% FBS. Cells were maintained in the incubator at 37°C and cultured for further 3 days, then cell viability was investigated by alamarBlue assay. For the complete experiment, MDA-MB-231 or HDFas as healthy control were seeded in 24-well plates (1.5 x 10^4 cells/well) for the 2D static control and cultured in complete medium for 24h. Then, medium was removed, and cells were treated with 1 mL of No glucose, Low glucose or High glucose-containing medium, supplemented with 10% FBS and 1% P/S. Cells were further cultured in static condition, at 37°C and 5%CO_2 for 3 days. In parallel, 3D cancer and healthy models were prepared as described above and cultured for 24 h prior to the start of the experiment. After 24 h, 3D gels were either moved in 24-well plate for static culture or in MIVO® Single Flow for dynamic culture and treated with gel culture medium with different glucose levels (No G, Low G and High G culture medium supplemented with 10% FBS, 1% P/S and 5 mM $CaCl_2$) for 3 days. Each well of static culture was treated with 1 mL of culture medium, while each MIVO® was filled with 250 µL in the apical compartment and about 3.5 mL in the basal circuit. The peristaltic pump was set to guarantee a flow rate of 1 mL/min. Both 2D and 3D models were maintained in incubator at 37°C and 5% CO_2 for three days treatment (time point T3). Further characterization on the different experimental groups were subsequentially conducted. For both cancer and healthy control models passage 5 cells were used.

2.6. Drug treatment

The effects of a chemotherapeutic drug treatment on the tumor model, either in combination with or without glucose deprivation therapy (fasting) were studied. The chemotherapeutic drug used was Cisplatin CRS (Ph. Eur.). MDA-MB-231 or HDFas as healthy control were seeded in 24-well plates (1.5 x 10^4 cells/well) for the 2D static control and

cultured in complete medium for 24h. In parallel, 3D cancer and healthy models were prepared as described above and cultured for 24 h prior to start the experiment. After 24 hours, both 2D and 3D tumor models were pre-conditioned (T0) for further 24 hours in High glucose complete medium (High group) or in No glucose medium (fasting). More specifically, for the 2D static control medium was removed and cells were washed and treated with 1 mL of High glucose- (High group) or No glucose- (fasting) containing medium, supplemented with 10% FBS, 1% P/S and 5mM $CaCl_2$. In addition, 3D gels were either moved in 24-well plate for static culture or in MIVO® Single Flow for dynamic culture (2 gels in each MIVO®) and treated with High glucose- (High group) or No glucose- (fasting) containing medium, supplemented with 10% FBS, 1% P/S and 5mM $CaCl_2$. Each well of static culture was treated with 1 mL of culture medium, while each MIVO® was filled with 250 µL in the apical compartment and about 3.5 mL in the basal circuit. The peristaltic pump was set to guarantee a flow rate of 1 mL/min. After 24 hours (T1), medium was removed and, after a cell washing, replaced with treatment medium. Specifically, each of the two experimental groups was treated with 10 µM Cisplatin drug with or w/o glucose or left in the same culture medium as control. This led to the following six experimental groups: (i) High CTRL (High glucose for the entire culture); (ii) High + drug (pre-conditioning with glucose + Drug treatment with glucose); (iii) High + drug and Fasting (pre-conditioning with glucose + Drug treatment w/o glucose); (iv) Full Fasting (No glucose for the entire culture); (v) Fasting + High and drug (pre-conditioning w/o glucose + Drug treatment with glucose); (iii) Full Fasting + drug (pre-conditioning w/o glucose + Drug treatment w/o glucose).

After 24 h, cells were cultured in incubator at 37°C and 5% CO_2 for further 48 hours. Cells passage 5 were utilized both for tumor and healthy models. The managing of the different models was conducted within a biological hood to ensure sterile conditions.

2.7. Characterizations

At the end of the experiments, the respective *in vitro* models 2D static, 3D static, and 3D dynamic were subjected to further characterization.

2.7.1. Viability assay: AlamarBlue and Live&Dead

AlamarBlue. For a semi-quantitative analysis of cell viability as a terminal readout, the commercially available AlamarBlue assay (Invitrogen) was used. AlamarBlue is a resazurin-based assay acting as a cell health indicator by using the reducing power of living cells to quantitatively measure viability. Resazurin is a non-toxic, cell-permeable

compound that is blue in color and virtually non-fluorescent. Upon entering living cells, resazurin is reduced to resorufin, a compound that is red in color and highly fluorescent. Changes in viability can be easily detected using either an absorbance or fluorescence-based plate reader. Prior to sample preparation, a solution containing DMEM High glucose medium with 0% FBS and AlamarBlue reagent at a 1X concentration was prepared in a 15 mL Falcon tube. This reagent solution was prepared in a volume sufficient for the treatment of all the samples of interest and for blank control realization. The analysis was performed in duplicate on at least two independent experiments. The wells containing 2D cultures were washed with 0.9% NaCl physiological solution with 5 mM $CaCl_2$ to remove any residual FBS. Subsequently, 500 µL of reagent solution was added to each well. The cultures were then incubated at 37°C and 5% CO_2 for 3 hours. Hydrogels from both 3D static and 3D dynamic models were transferred using sterile tweezers and individually relocated into dedicated wells of a 24-well plate. Each well was washed with 0.9% NaCl physiological solution containing 5 mM $CaCl_2$ to remove any FBS residual. A volume of 500 µL of AlamarBlue solution was then added to each well. The cultures were incubated at 37°C and 5% CO_2 for 6 hours. Additionally, a blank control well, without any cellular models, was prepared by washing with 0.9% NaCl physiological solution containing 5 mM $CaCl_2$ and then adding 500 µL of the AlamarBlue reagent solution. At the end of the predetermined incubation time, 100 µL of the reduced reagent solution from each well were collected four times and transferred individually into a 96-well plate (VwR 96, flat) proceed with absorbance reading via spectrophotometer (Infinite® M Nano, Tecan) software (i-control™ 2.0, Tecan). Data were subsequently collected and processed to evaluate the percentage of reagent reduced by the cells present in the respective samples. Data values of each well were elaborated through (2.1):

$$\text{reduction} = [(Y_{570} - W_{570}) - (X_{600} - W_{600})] \times 100 \tag{2.1}$$

where W_{570} and W_{600} are average blank absorbance at 570 nm and 600 nm respectively whereas Y_{570} and X_{600} are the sample absorbance value at the same specific wavelengths. For better comparison between different experimental groups, reduction was expressed as percentages relative to the control (HIGH CTRL) by the following equation (2.2):

$$\text{cells viability (\% CTRL)} = \frac{reduction_{sample}}{\hat{reduction}_{CTRL}} \times 100 \tag{2.2}$$

The entire handling of the models and sample collection was conducted under sterile conditions within a biological hood. Additionally, to protect the reagent from potential damage caused by visible light, exposure to light sources during AlamarBlue solution

handling was minimized.

Live&Dead. To perform this fluorescence-based viability assessment, a commercial reagent, the Live and Dead Cell Assay (ab115347), produced by Abcam (Abcam Limited, USA), was employed. Initially, a reagent solution was prepared according to the manufacturer's protocol, with an excess volume to ensure adequate coverage for all the samples of interest. Specifically, the solution was obtained by diluting Cell Dye II/Live Cell Staining Dye 2:1000 (2 µL/mL) and Dead Cell Staining Dye 1:1000 (1 µL/mL) in Assay Buffer XXVII/Assay Buffer to perform the assay on 2D samples. For the 3D cell-laden hydrogels, the solution was prepared using the same staining dyes concentrations in Assay Buffer XXVII/Assay Buffer calcium enriched (5 mM $CaCl_2$). For the 2D models, the assay was performed on one well per experimental group. After media remotion, 300 µL of the pre-warmed reagent solution was added, followed by incubation for 15 minutes at 37°C. At the end of incubation step the wells were then directly observed with inverted fluorescence microscope (Nikon Eclipse Ts2-FL). Live cells appeared green ($\lambda ex/\lambda em$ = 495/519 nm), while dead cells appeared red ($\lambda ex/\lambda em$ = 546/647 nm). Multiple images were acquired for each sample using the dedicated software (X-Entry, Alexasoft). For the 3D samples, one gel per experimental group was transferred using sterile tweezers into an individual well of a 96-well round-bottom plate (Euroclone). Each well received 100 µL of the pre-warmed reagent solution, prepared as described earlier, and incubated at 37°C for 15 minutes. After incubation, the Live and Dead assay reagent was removed, and wells washed with 0.9% NaCl physiological solution containing 0.5 mM $CaCl_2$. The hydrogels were then transferred manually onto glass slides and observed under fluorescence microscope for image acquisition, following the same procedure as for the 2D samples. Throughout the handling of samples and reagents, sterile conditions were maintained. Furthermore, during procedures involving the dyes, exposure to intense light sources was minimized.

2.7.2. Immunostaining

Immunostaining was conducted to assess the expression of cellular proliferation and hypoxia markers, specifically Ki67 and HIF-1α. For both 2D and 3D cultures, staining was performed on a single sample for each Fasting simulation experiment, on two independent experiments.

2D models staining. After remotion of the treatment media, cells were washed with PBS and fixed by adding 4% (v/v) formaldehyde (formalin) at room temperature for

15 minutes, under a chemical hood. The fixation solution was then removed, and any residuals were washed off with two rinses in PBS. The cellular models were permeabilized with 0.1% Triton X-100 in physiological solution to allow access to intracellular proteins. After 15 minutes incubation at room temperature, cell were washed twice with PBS and incubated for 1 hour at room temperature with a blocking solution containing 2% (w/v) bovine serum albumin (BSA) in 0.9% NaCl, to prevent the non-specific binding of secondary antibody. After removing the blocking solution, the cell culture models were washed twice and then incubated overnight at 4°C with the mix of primary antibodies. Mix of primary antibodies was prepared by adding rabbit anti-human Ki67 (ab15580, abcam) (1:1000) and mouse anti-human HIF-1α (ab1, abcam) (1:200) to a 0.2% BSA solution in 0.9% NaCl. To avoid solution evaporation the 24-well plate was sealed with parafilm before being placed in the refrigerator. The following morning, after three washes, the cell culture models were incubated with the mix of secondary antibodies. Mix of secondary antibodies was prepared by adding goat anti-rabbit AlexaFluor488 (1:200) and goat anti-mouse AlexaFluor555 (1:200) to a 0.2% BSA solution in 0.9% NaCl. The samples were incubated at room temperature for 1 hour and then rinsed three times. Therefore, a nuclei control staining was achieved by 15 minutes incubation with 1 µM DAPI in physiological solution. Before proceeding with samples examination under fluorescence microscope, samples were washed twice with physiological solution.

3D models staining. 3D hydrogels were first manually transferred using sterile tweezers into a 96-well round-bottom plate before proceeding. The 3D cell-laden gels were washed with physiological solution 0.9% NaCl with 5 mM $CaCl_2$ and fixed with 4% (v/v) formaldehyde (formalin) in 0.9% NaCl solution containing 1 mM $CaCl_2$, at room temperature for 15 minutes, under a chemical hood. Following, the fixation solution was removed, and any residuals were discarded through a double wash. 3D cellular models were subjected to a permeabilization step with 0.1% Triton X-100 in 5 mM $CaCl_2$ saline solution. After 2 hours incubation at room temperature, the permeabilization solution was disposed, followed by two rinses with washing solution 5 mM $CaCl_2$. Consequently, non-specific secondary antibodies were blocked by adding blocking solution containing 2% (w/v) bovine serum albumin (BSA) in 0.9% NaCl with 5 mM $CaCl_2$. Samples were incubated at room temperature for 2 hours before proceeding with the remotion of the blocking solution by a double rinse. Afterward, cell culture models were incubated overnight at room temperature with a mix of primary antibodies. Specifically, rabbit anti-human Ki67 (ab15580, abcam) (1:1000) and mouse anti-human HIF-1α (ab1, abcam) (1:200) in a 0.2% BSA solution in 0.9% NaCl with 5 mM $CaCl_2$. The 96-multiwell was sealed with parafilm to control solution evaporation. The day after, next three washes the samples were incu-

bated with the mix of secondary antibodies. Mix of secondary antibodies was prepared by adding goat anti-rabbit AlexaFluor488 (1:200) and goat anti-mouse AlexaFluor555 (1:200) to a 0.2% BSA solution in 0.9% NaCl with5 mM $CaCl_2$. The samples were incubated for 2 hours in the dark at room temperature. Subsequently secondary solution remotion, they were rinsed three times with 5 mM saline solution before proceeding with 30 minutes incubation with 1 µM DAPI physiological solution 5 mM $CaCl_2$ to obtain control nuclei staining. After that, samples were rinsed two additional times and moved manually on a coverslip carefully to maintain preserved the gels' structure and then visualize them under fluorescence microscope.

2.8. Statistical analyses

Data were analyzed with GraphPad Prism 9.3 software. Two-way ANOVA was used for cells viability measurement comparison between the different experimental groups. Level of significance was set at $p < 0.05$ (*$p < 0.05$, **$p < 0.01$, ***$p < 0.001$, ****$p < 0.0001$). Number of replicates for each experiment are reported in figure legends. Data are shown as mean ± SD.

3 | Results and Discussion

3.1. Different concentrations of Fetal Bovine Serum do not influence cell responses to fasting *in vitro*

The final aim of current study is to evaluate the effects of fasting, meant as glucose starvation, on an *in vitro* tumor model, by modulating the amount of glucose available to the tumor cells. However, the conditions to which the cells are exposed *in vitro* significantly differ from those *in vivo*. The availability and types of circulating nutrients and metabolites indeed extend beyond glucose, including proteins, lipids, vitamins, and other compounds. Standard *in vitro* culture procedures require fetal bovine serum (FBS) as one of the key components supplying the essential metabolites and nutrients required by cells. FBS is supplemented into the culture medium and, although its composition may vary due to lots of variability, it generally provides cells with a nutrient-rich environment, necessary for their support and growth [88]. To achieve a biomimetic emulation of fasting conditions comparable to those *in vivo*, it is therefore essential to investigate the role of FBS within *in vitro* fasting protocols. Specifically, it is essential to determine whether fetal bovine serum plays any role in modeling the *in vitro* fasting conditions. To answer this question, a preliminary experiment was conducted in a first optimization step to investigate the effect of different FBS concentrations on 2D cell culture, with different glucose levels. MDA-MB-231 were treated with DMEM High glucose (High G), DMEM Low glucose (Low G) or DMEM No glucose (No G), supplemented with 0%, 2%, 5% or 10% FBS Figure 3.1A. Cell viability was investigated by AlamarBlue assay after 3 days Figure 3.1B.

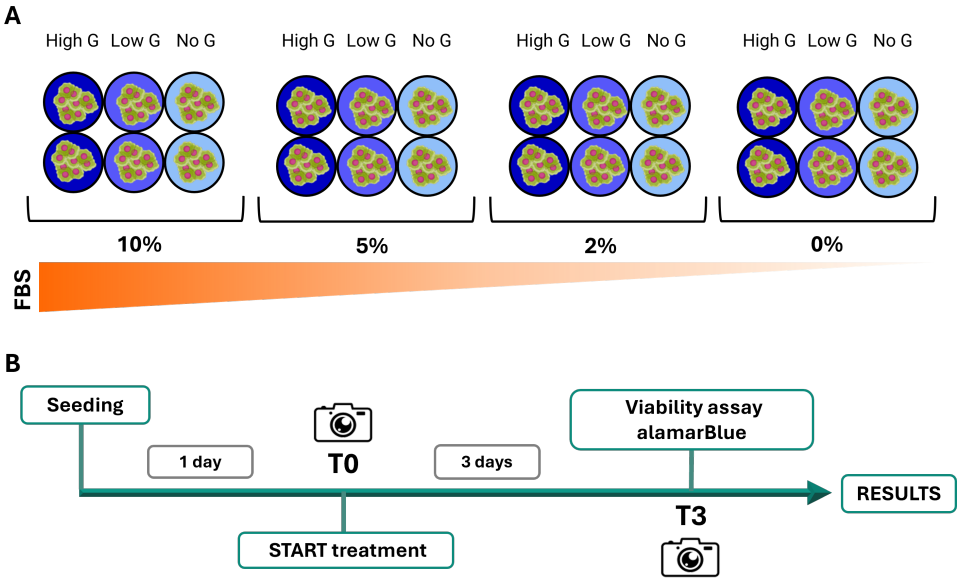

Figure 3.1: Experimental setup with different FBS concentrations in fasting conditions. (A) Time line of the experiment. (B) Schematic representation of the experimental groups.

A qualitative assessment of the cells through microscopic observation, as illustrated in Figure 3.2A, revealed that among groups supplemented with different concentrations of FBS, cellular distribution and morphology were consistent across samples treated with equivalent glucose concentrations. In both the High Glucose (High G) and Low Glucose (Low G) groups, the cells were more abundant, adherent, and spread. In contrast, the glucose-free groups exhibit visibly fewer cells predominantly rounded and poorly adherent. Additionally, cells cultured without FBS showed a marked increase in dead and detached cells, leading to a reduced number of adherent and spread cells. Notably, a decline in cellular conditions was qualitatively evident as glucose availability decreases, particularly in the group treated with 0% FBS and devoid of glucose in the culture medium. These qualitative morphological observations aligned with the semi-quantitative analysis of cellular viability obtained via the alamarBlue assay. As reported in Figure 3.2B, cellular viability, expressed as percentage of control group (High G, 10% FBS), was consistently higher in samples treated with High G and Low G, regardless of variations in FBS concentrations. Conversely, the No Glucose (No G) groups exhibited an approximate 50% reduction in viability compared to the control. Finally, in samples cultured without FBS, viability was further reduced by half, even in cells cultured in High G and Low G. Moreover, comparative analysis of glucose treatments (High G, Low G, and No G) across different FBS concentrations showed no significative difference. Overall, the assessment of both qualitative and semi-quantitative findings related to morphology and viability indicates that glucose availability significantly affects cellular behavior, independently of

FBS concentrations.

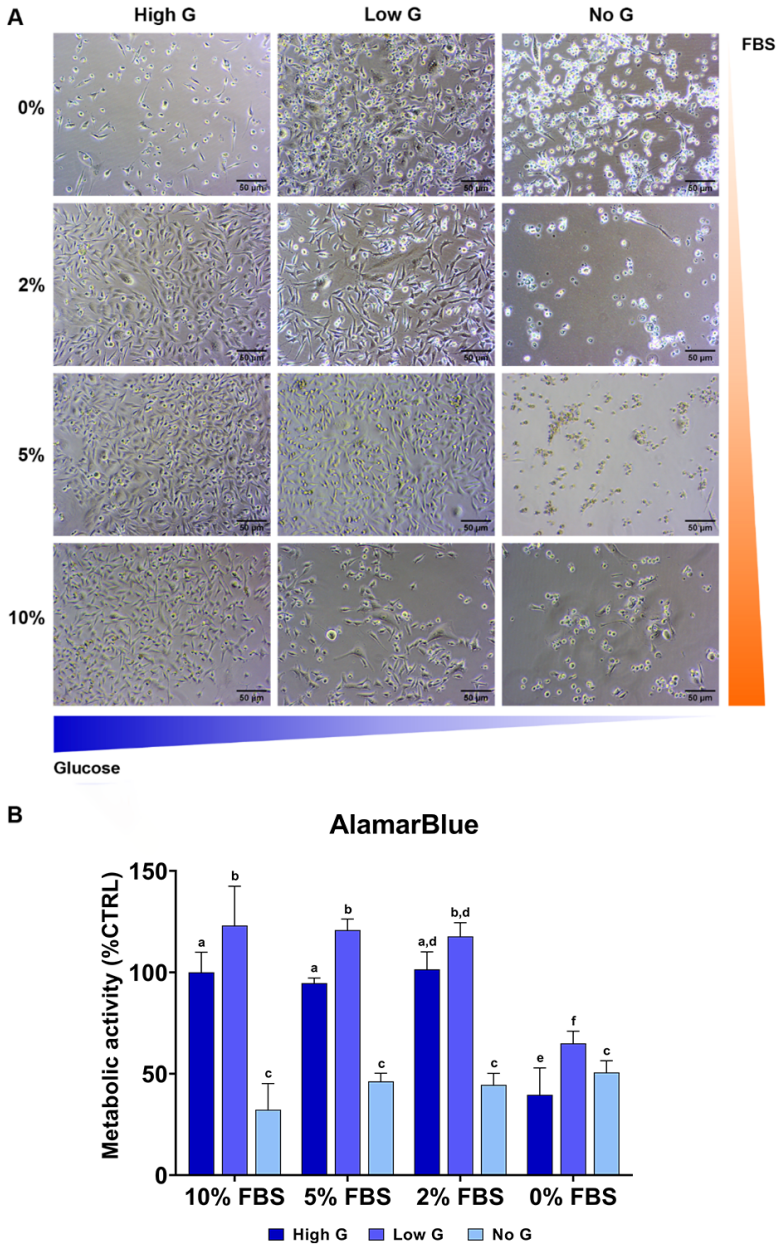

Figure 3.2: Effects of different FBS concentrations in fasting conditions. (A) Representative images of MDA-MB-231 cells cultured in DMEM High glucose (High G), DMEM Low glucose (Low G) or DMEM No glucose (No G), supplemented with 0%, 2%, 5% or 10% FBS. Scale bar: 50 µm. (B) Cells viability by AlamarBlue assay. Data are reported as mean ± S.D. and expressed as percentage of Control (High G,10% FBS). Values with shared letters are not significantly different ($P > 0.05$) according with two-way ANOVA. N=2.

Specifically, the High G and Low G groups displayed similar treatment responses, characterized by comparably high viability values. In contrast, the No G groups showed a

distinct negative impact on cell viability attributable to fasting. The 0% FBS group can be considered an exception, where the differences among glucose treatments are less pronounced. This phenomenon is likely due to the overarching detrimental effect of FBS deprivation, regardless of glucose levels, leading to a deficiency in essential nutrients required for cellular growth and proliferation. Based on these findings, it can be concluded that the effects of glucose deprivation are largely independent of FBS and its concentration. Therefore, in subsequent experiments, culture media enriched with 10% FBS were utilized for both control and treatment groups.

3.2. Glucose deprivation reduced metabolic activity in both 2D and 3D cancer models

The focus of this investigation is to better understand how nutritional variations in the tumor microenvironment may influence the progression of aggressive malignancies, such as triple-negative breast cancer (TNBC). Specifically, we aimed to explore the potential response of tumor tissue to the reduction or deprivation of circulating glucose. Most of the *in vitro* available studies rely on 2D models, to investigate tumor responses to fasting or starvation. However, these 2D standard models are not fully reliable for accurately reflecting the *in vivo* physiological conditions of tumors. In this scenario, the use of 3D models is essential for mimicking the real tumor microenvironment, enabling a more accurate representation of cellular behaviors and responses to nutritional changes.

To achieve this, in the present study, glucose levels were modulated in both 2D and 3D *in vitro* cancer models, to assess the effects on key parameters such as cell viability, proliferation, and hypoxia. In this comprehensive experiment, MDA-MB-231 cells were seeded in static 2D models as well as in 3D models created using three-dimensional alginate-based hydrogels. Alginate offers several advantages as a material for 3D *in vitro* models, particularly due to its versatility in creating hydrogels with tunable stiffness. This allows the development of gels that support nutrient penetration and the potential migration of tumor cells, which is crucial for simulating the tumor microenvironment. The mechanical properties of these gels can be indeed precisely controlled through calcium ion-mediated crosslinking, offering a high level of customization. Furthermore, its ability to form stable 3D structures over extended periods makes alginate an excellent candidate for *in vitro* pharmacological testing models [89]. In a previous study, the utility of 3D alginate gels in cultivating lowly aggressive breast cancer cells (e.g., MCF-7 cell line), exploring their viability, proliferation, and morphological organization was demonstrated [90]. The optimal composition of alginate and calcium was determined to enhance cell activity, and

the 3D model effectively replicated the cluster-like organization and round morphology typical of less invasive cancer cells. Finally, the use of alginate-based 3D models allows to maintain a balance between complexity and simplicity, ensuring retaining of key features of the tumor microenvironment without obscuring the data, thus allowing for clear and straightforward interpretation of the results. Inertness, chemical stability, and lack of intrinsic bioactivity allow indeed to better focus on the treatment mechanisms and tumor responses [91].

Three-dimensional breast cancer models were used in this study and cultured in both static and dynamic conditions. The previously developed MIVO® Single Flow millifluidic device was adopted for the culture of 3D breast cancer models under dynamic conditions Figure 3.3. Flow rate of 1 mL/min in the range of physiological velocities was recapitulated in a closed circuit. MIVO® fluidic device has been already reported to allow culture of clinically relevant sized cancer models, and to resemble the human circulation and drug diffusion to reach the tumor mass.

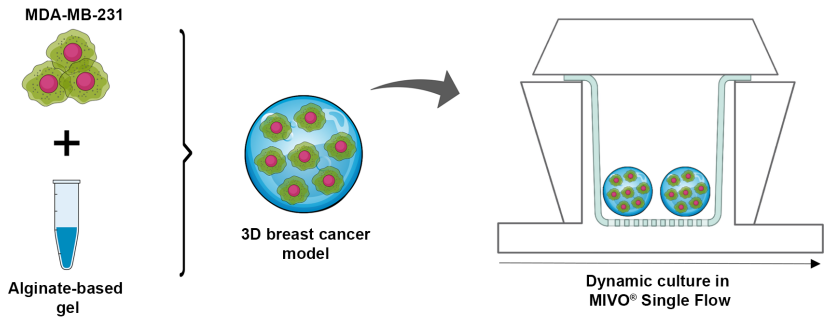

Figure 3.3: Schematic of cell-laden hydrogel realization and 3D dynamic model within MIVO® Single Flow.

All models were cultured in DMEM High Glucose (High G), DMEM Low Glucose (Low G), or DMEM No Glucose (No G) (Figure 3.4A). After three days, cellular viability was assessed based on metabolic activity using the AlamarBlue assay, and live/dead cell distribution was compared through a fluorescence-based Live and Dead assay. Additionally, immunostaining provided specific functional insights into cell proliferation and hypoxia across the different samples (Figure 3.4B).

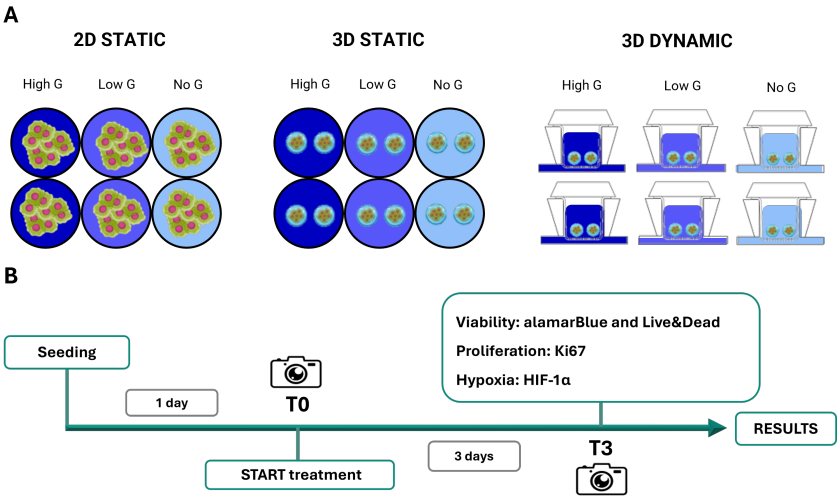

Figure 3.4: Experimental setup with different *in vitro* models in fasting conditions.(A) Schematic representation of experimental groups within 2D static, 3D static, and 3D dynamic *in vitro* models. (B) Timeline of the experiment.

Microscopic analysis of the 2D models, shown in fig. 3.5A, confirmed previous observations. As glucose levels decreased, cellular cultures exhibited reduced replication after three days. Notably, fewer cells were observed in groups with glucose levels lower than the control (High G). Among all samples, the No G treatment led to a significantly reduced cell proliferation, with a higher proportion of dead, detached, and rounded cells. In the 3D models, cells embedded within the polymeric matrix could be distinguished by their typically rounded morphology, based on images captured under optical microscope (fig. 3.5A). However, no significant visual difference was observed between the 3D models across experimental groups. Metabolic activity results for the static 2D models are partially consistent with preliminary morphological observations. As depicted in fig. 3.5B, experimental groups supplied with glucose showed greater cellular viability. In contrast, samples treated with glucose-free culture medium (No G) exhibited approximately 50% lower viability compared to the control. No significant difference was found between the Low G group and the High G control. These results are in line with data reported in literature, where glucose deprivation was demonstrated to reduce cancer cell proliferation motility and metabolic activity [92, 93]. The trend observed in the 2D static model was similarly replicated for both the static and dynamic 3D models. However, it is important to underline that both static and dynamic 3D models showed slightly higher cell viability under glucose-free conditions compared to 2D models, which aligns with previous studies suggesting that 3D models exhibit greater resistance to treatments, including chemotherapy, compared to 2D standard models [94–96]. These results suggest that glucose deprivation significantly reduces cell proliferation and metabolic activity in both 2D

and 3D models, but 3D models show greater resistance to nutrient deprivation. This indicates that 3D models may provide a more realistic representation of cellular responses to nutrient scarcity, compared to 2D models, which fail to fully reflect the complexity of the tumor microenvironment.

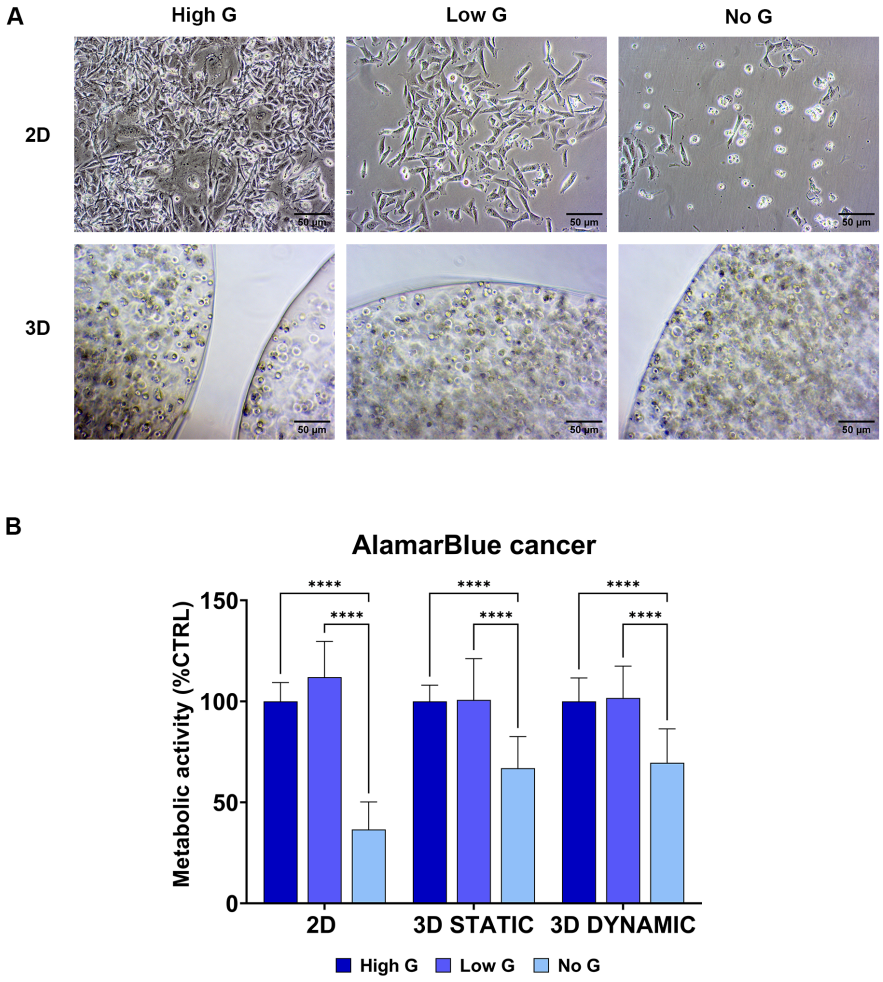

Figure 3.5: Effects of glucose deprivation on cancer cell metabolic activity. (A) Representative images of MDA-MB-231 cells both in 2D and 3D condition cultured in DMEM High glucose (High G), DMEM Low glucose (Low G) or DMEM NO glucose (No G). Scale bar: 50 µm. (B) Cells viability by AlamarBlue assay. Semi-quantitative data are reported as mean ± SD and expressed as percentage of Control (High G). Statistical comparison was made using two-way ANOVA (N=4), *P<0.05, **P<0.01, ***P<0.001, and ****P<0.0001.

3.3. Glucose deprivation increased cell death and reduced cell proliferation in both 2D and 3D cancer models

Glucose plays a pivotal role in supporting cancer cell proliferation by providing both energy and metabolic intermediates necessary for growth. Elevated glucose availability enhances the rate of cell division, while glucose deprivation has been reported to inhibit cell growth, inducing cellular stress and ultimately limiting tumor expansion [92]. To better understand the effects of glucose deprivation, its effect on cell viability was further analyzed by Live & Dead assay. The Live/Dead assay, which distinguishes live cells (stained green) from dead cells (stained red), yielded results in the 2D models that align with qualitative observations from optical microscopy. In the High Glucose (High G) group, a substantial number of viable cells were evident, accompanied by a lower frequency of dead cells (Figure 3.6A). Conversely, in the Low Glucose (Low G) and No Glucose (No G) groups, a clear negative trend was observed, with a marked reduction in viable cells and a corresponding increase in cell death. The No G group, in particular, demonstrated a significantly higher signal of dead cells compared to live cells. Furthermore, among the surviving cells in the No G group, a noticeable decrease in cellular elongation and spreading was qualitatively observed compared to the other experimental groups, indicating impaired cellular morphology under glucose deprivation.

The images presented in Figure 3.6B-C, depicting the Live & Dead assay for static and dynamic 3D models, qualitatively demonstrated a generally homogeneous distribution of live cells across all experimental groups. These cells exhibited a predominantly rounded morphology, consistent with observations made through visible light microscopy (Figure 3.6A). In contrast, dead cells were more prevalent in groups subjected to glucose deprivation, with the No Glucose (No G) group in the dynamic 3D model showing the highest distribution of dead cells among all samples. Variations in the size and shape of fluorescence signals in the 3D samples are likely attributable to cells located in different z-planes during image acquisition, providing further evidence of the three-dimensional structure of the cultures. From a viability standpoint, the fasting (No G) treatment consistently yielded the lowest viability across all experimental models. The observable differences between the 3D and 2D models can potentially be attributed to the complexity of the 3D model itself. The presence of a three-dimensional matrix may influence the metabolic plasticity of tumor cells, promoting the activation of alternative metabolic pathways to glycolysis [97]. This demonstrates an increased biomimetic response in the

3D model compared to the standard 2D culture. Furthermore, the distribution and morphology of live and dead cells suggest that the No G treatment not only suppresses tumor cell proliferation but also increases the number of dead and possibly apoptotic cells, which is in agreement with data already reported in literature [98–100].

In contrast, the results for the Low Glucose (Low G) treatment were comparable to the High Glucose (High G) control, regardless of the complexity of the tumor model. Both the viability percentages and fluorescence images from the Live & Dead assay showed no significant difference between these groups. This suggests that a reduction in glucose alone did not substantially affect the tumor models under investigation. These findings are consistent with previous studies that have reported limited effects and, in some cases, tumor resistance under reduced glucose conditions [98].

To further assess the proliferation and hypoxia status of cells within the samples, immunostaining was performed. Specifically, the expression of the nuclear protein Ki67, associated with active phases of the cell cycle and therefore proliferation, as well as HIF-1α, a subunit of the HIF-1 transcription factor that acts as a primary regulator of cellular response to hypoxia, were investigated. As shown in Figure 3.65, nearly all cells in the 2D models were positive for Ki67 across all experimental groups, indicating active proliferation. In contrast, hypoxia was more pronounced in the Low Glucose (Low G) and No Glucose (No G) groups, with reduced hypoxic conditions observed in the control group. Interestingly, under fasting treatment, cells exhibited co-expression of both Ki67 and HIF-1α, suggesting that cells may be attempting to proliferate while also activating stress response pathways to manage with the lack of glucose. This dual response could reflect a form of metabolic adaptation, where cells are trying to survive and maintain growth under adverse conditions, potentially contributing to increased resistance to therapies that target glucose metabolism alone.

In the 3D model groups, both proliferation and hypoxia were observed, though to a lesser extent compared to the 2D models. Notably, instances of Ki67 positivity and co-expression of both Ki67 and HIF-1α were detected in all the experimental groups, in both static and dynamic conditions, indicating a more complex cellular response in the three-dimensional context. However, although less evident compared to 2D static culture conditions, a higher number of double-positive cells was observable in No G culture conditions, compared to both Low G and High G. As mentioned, the co-expression of both Ki67 and HIF-1α may suggest increased tumor cell aggressiveness and enhanced resistance to stress conditions. Ki67, as a marker of proliferating cells, and HIF-1α, a key regulator of cellular responses to low oxygen, are often co-expressed in aggressive tumors. This dual upregulation can reflect a heightened ability of tumor cells to proliferate rapidly while

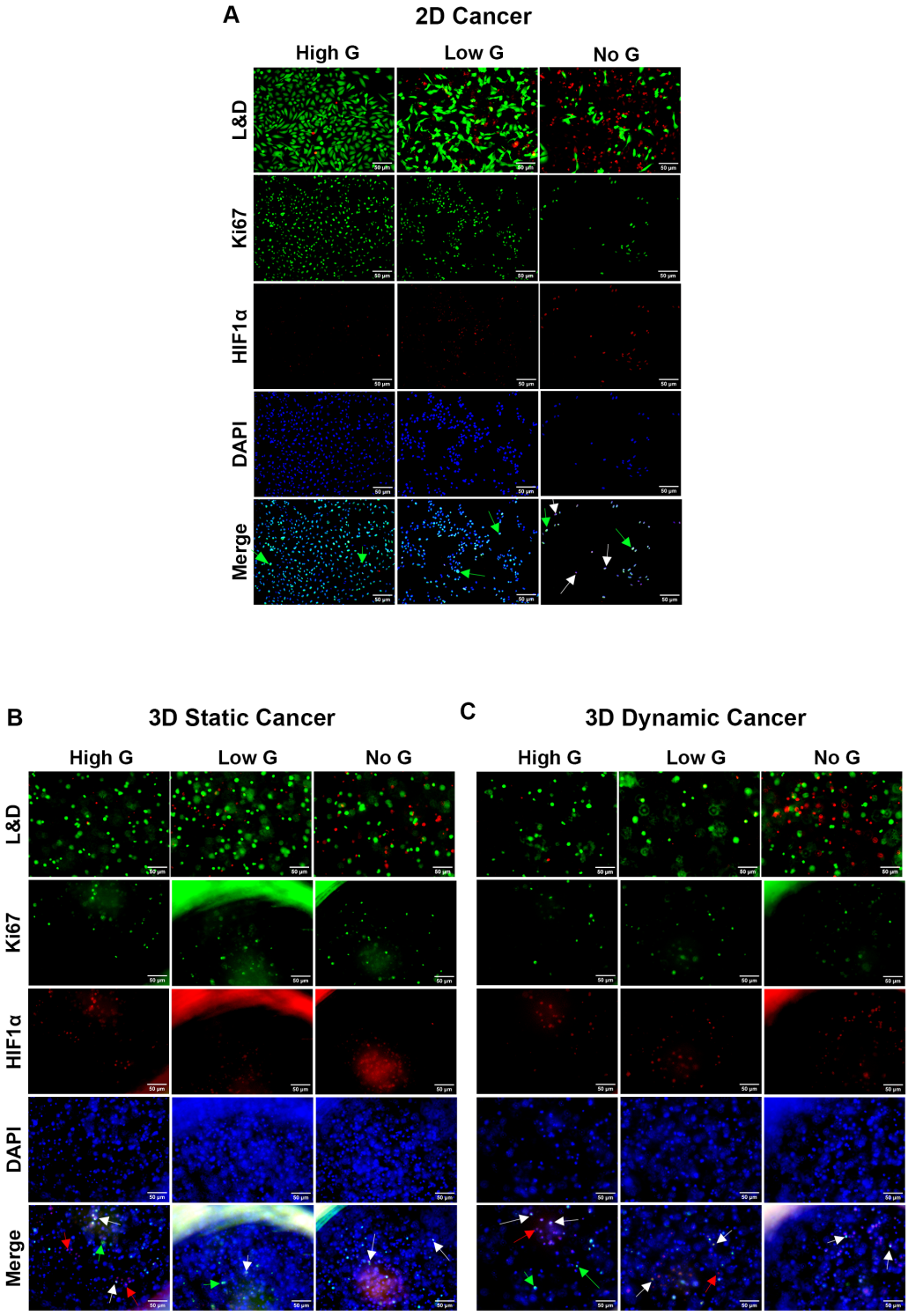

Figure 3.6: Cancer cells viability, proliferation and hypoxia. Representative images of Live & Dead staining and immunostaining of ki67 and HIF1α on 2D static (A) 3D static (B) and 3D dynamic cancer models (C). Scale bar: 50 µm. Green, red and white arrows point out ki67+, HIF1α+ and double-positive cells, respectively.

simultaneously adapting to the stress of a hypoxic microenvironment. Several studies have indeed established a correlation between the co-expression of Ki67 and HIF-1α and increased tumor aggressiveness, particularly in cancers like breast cancer [101]. Tumors exhibiting this marker profile tend to show more aggressive behavior, including accelerated proliferation, angiogenesis (the formation of new blood vessels to support tumor growth), increased tumor size, and a higher propensity for metastasis [102]. Moreover, these tumors often demonstrate resistance to conventional therapies, such as chemotherapy and radiation, due to their ability to adapt to nutrient and oxygen deprivation, thus limiting the efficacy of treatment regimens. These aggressive tumor characteristics are associated with poorer prognosis and reduced patient survival rates, as tumors that can maintain growth and spread under harsh conditions are more difficult to treat and control [103]. Finally, activation of the HIF-1α signaling pathway under glucose deprivation has beend already reported to lead to the acquisition of anti-apoptotic properties in human colon cancer cells [104].

Our findings highlight the critical role of glucose metabolism in tumor cell viability and proliferation. While glucose deprivation, particularly in the No Glucose (No G) group, significantly impaired cell survival, it also induced a complex response involving both proliferation and hypoxia, particularly in the 2D models. The 3D models, with their more biomimetic nature, exhibited a milder response, suggesting that tumor cells in more complex environments may engage alternative metabolic pathways to cope with stress. Moreover, the 3D model reliability in simulating the *in vivo* tumor microenvironment adds substantial value to these findings, as it better reflects the metabolic plasticity and cellular interactions observed in real tumors.

3.4. Glucose deprivation impaired healthy cell viability in 3D model but not in 2D standard culture

Fasting and caloric restriction have been widely studied for their effects on tumor cells, but their impact on non-pathological tissues remains less understood. Investigating these treatments in healthy tissue models is essential to better understand their broader physiological effects and to assess their potential benefits and risks in clinical settings. To explore this, an experiment was conducted using *in vitro* models of healthy tissue, aiming to evaluate how these treatments, previously analyzed in the tumor context, influence cellular viability in a non-pathological setting. This approach provides valuable insights into the potential impact of targeted dietary interventions on healthy tissues, offering a basis for balancing the benefits and risks of such strategies in clinical applications.

In this study, the response of a healthy tissue model subjected to glucose modulation treatments, similar to those applied in the previous tumor model, was evaluated. For this purpose, human dermal fibroblast (HDF) cells were cultured in 2D static, 3D static, and 3D dynamic models, designed to mimic the same conditions of the TNBC model. Each experimental group was cultured in DMEM High Glucose (High G), DMEM Low Glucose (Low G), or DMEM No Glucose (No G). Following a three-day treatment period, the samples were subjected to morphological analysis through optical microscopy, and cell viability was assessed using both Live&Dead and AlamarBlue assays to evaluate the impact of glucose modulation on cellular health in a non-pathological context.

Optical microscopy images shown in Figure 3.7A indicated a high degree of proliferation in both the Low G and control High G groups, characterized by numerous adherent and elongated cells. This morphology aligns with the typical features of bidimensional fibroblast cultures. Moreover, the cells were densely packed and elongated along specific directions, further reinforcing the observation of healthy condition. A similar scenario was observed in the experimental group subjected to glucose deprivation (No G). Although the cell density appeared lower compared to the previous two groups, the cells remained well adherent and elongated, with no apparent signs of rounding or detachment indicative of dead cells. From Live & Dead assay results, in all experimental groups, live cells predominated, with no visible accumulation of dead cells, as evidenced by the absence of red fluorescence, suggesting overall cell viability across all conditions.

For the three-dimensional models, the Live & Dead assay images shown in Figure 3.7B revealed no significant qualitative differences between dynamic and static cultures. A consistent distribution of live cells (in green) was observed across all experimental groups, with a slightly increased presence of dead cells (in red) in the No G treatment groups.

The qualitative findings from the Live & Dead assay and morphological analysis were consistent with the semi-quantitative viability data obtained via the AlamarBlue assay. Specifically, the metabolic activity of the cells, evaluated at the end of the treatments, corroborated the preliminary observations, as shown in Figure 3.7C. In the 2D cultures, similar viability levels were recorded across all experimental groups, indicating that the glucose modulation treatments did not adversely affect cellular metabolic activity.

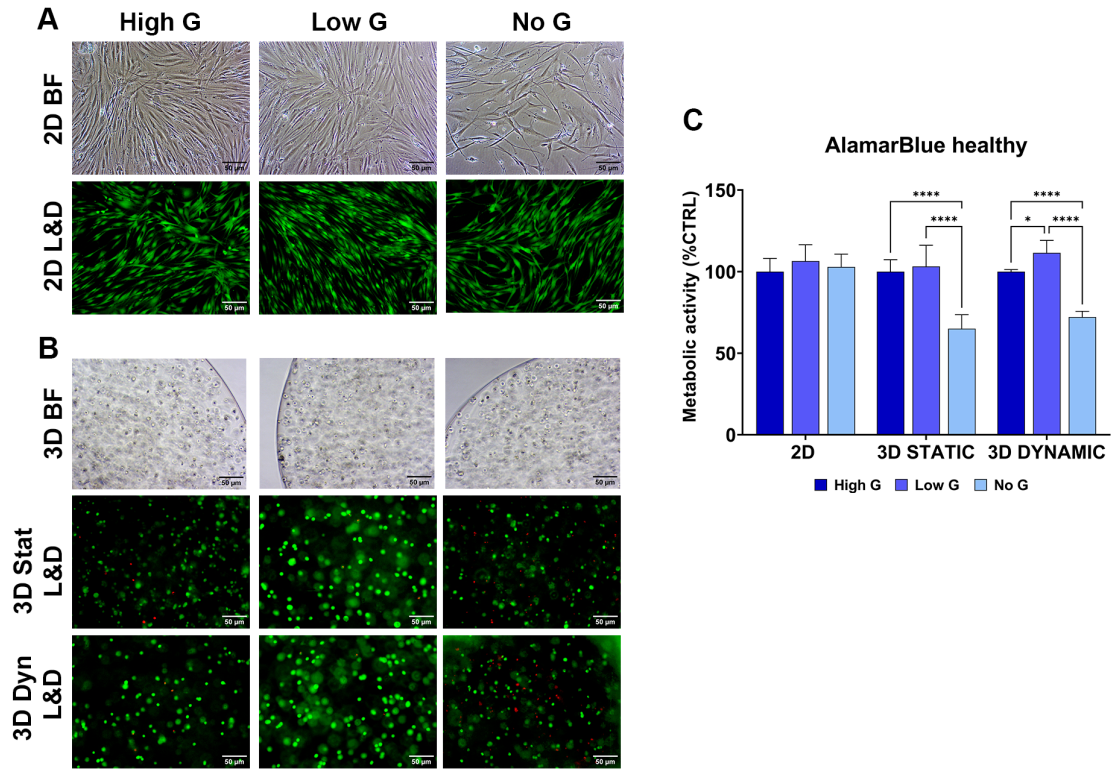

Figure 3.7: Effects of glucose deprivation on healthy cell viability. Representative images of HDFs cells and Live & Dead staining both in 2D (A) and 3D (B) condition cultured in DMEM High glucose (High G), DMEM Low glucose (Low G) or DMEM NO glucose (No G). Scale bar: 50 µm. (C) Cells viability by AlamarBlue assay. Semi-quantitative data are reported as mean ± SD and expressed as percentage of Control (High G). Statistical comparison was made using two-way ANOVA (N=4), *P<0.05, and ****P<0.0001.

This stands in stark contrast to the results obtained from the static 2D cultures of the tumor model, which exhibited a markedly negative response to glucose deprivation (Figure 3.7). The discrepancy between the static 2D cultures of healthy fibroblasts and the tumor model can be attributed to the inherent differences in cellular behavior and metabolic adaptability between normal and cancerous cells. In the static 2D cultures of human skin fibroblasts, cells seem capable of adapting to glucose reduction by adjusting their metabolic activities, including downregulating non-essential processes to survive in a low-glucose environment [105]. This adaptation can lead to a state of cellular stress or senescence, which results in a decrease in proliferation [106] but does not necessarily cause cell death, as observed in the Live&Dead and AlamarBlue assays. In contrast, tumor cells are often more dependent on glycolysis (even under aerobic conditions), which makes them less adaptable to glucose deprivation.

Conversely, in the 3D models, under both static and dynamic conditions, a notable re-

duction in viability was observed in the glucose-deprived (No G) samples compared to the control, while no significant differences were detected between the control and the glucose-restricted (Low G) groups, suggesting that moderate glucose reduction did not impact cell viability in the same way as complete glucose deprivation and showing consistency with data observed in tumor cells. The heightened sensitivity observed in the 3D model under glucose deprivation suggests that healthy tissues may struggle to maintain proper function when glucose levels are severely restricted. The reduced viability in these samples compared to 2D standard group could be due to the increased complexity of the 3D model, which better reflects the *in vivo* environment. *in vivo*, if glucose is withdrawn from healthy tissues, especially over an extended period, cells could experience metabolic stress and be forced to shift to alternative energy sources, such as fatty acids or amino acids. However, this metabolic shift is not as efficient as glucose metabolism and could impair cell function, leading to reduced proliferation and tissue dysfunction over time. In certain tissues, such as the brain and muscles, glucose is a critical energy source, and prolonged deprivation could result in severe consequences, including cell death, organ dysfunction, or loss of tissue integrity [107].

These findings underscore the potential risks of dietary interventions, like fasting or caloric restriction, which may have detrimental effects on healthy tissues, particularly in the context of chronic or severe glucose restriction. Therefore, a careful balance must be maintained to ensure that while targeting tumor cells, healthy tissues are not adversely affected [105, 106].

3.5. Synergistic Effects of Chemotherapy and Fasting in Breast Cancer Models

Glucose serves as the primary energy source for the human body and plays a crucial role in the physiology of cancer cells. Under conditions of hypoxia and glucose scarcity, cancer cells exhibit metabolic plasticity by autonomously shifting their glucose metabolism toward aerobic glycolysis. This metabolic reprogramming is tightly regulated by a network of molecular factors, allowing cancer cells to sustain proliferation even under metabolic stress.

However, multiple studies have demonstrated that cancer cells can develop adaptive mechanisms to tolerate glucose deprivation, complicating the therapeutic potential of this approach. Such mechanisms may involve the activation of alternative metabolic pathways and the modulation of stress responses that enhance cell survival. Final aim of this study

was to elucidate the potential effects on a tumor model arising from the combination of chemotherapy agents and dietary interventions. Specifically, the synergy between cisplatin, a well-established antiproliferative agent, and fasting was investigated. Consistent with previous studies, fasting was simulated *in vitro* by treating the respective samples with glucose-free culture media. Furthermore, to gain insights into the influence of tumor microenvironment complexity, this study was conducted in parallel in 2D static, 3D static and 3D dynamic cancer models. Since previous experiments demonstrated that, across all *in vitro* models studied, irrespective of their complexity, treatment involving a reduction in glucose availability (Low G) did not lead to adverse impacts on viability, either in pathological tumor models or in healthy ones, only complete glucose deprivation (named as fasting) was used in combination with drug treatment.

MDA-MB-231 cells were used to generate 2D Static, 3D Static, and 3D Dynamic breast cancer models. Both the 2D and 3D models underwent a pre-conditioning phase. Specifically, samples were divided into two experimental groups and cultured either in DMEM high glucose (High G) or DMEM no glucose (No G) to simulate fasting. On the subsequent day, the samples from the two main experimental groups were treated with cisplatin either in the presence or absence of glucose, or cultured with the same medium as in the pre-conditioning phase. This resulted in six distinct experimental groups (fig. 3.8):
(I) High CTRL (High glucose for the entire culture) representing untreated conditions and a standard diet, serving as a control for comparison;
(II) High + High and drug (pre-conditioning with glucose + drug treatment with glucose), representing chemotherapy without dietary modifications;
(III) High + Fasting and drug (pre-conditioning with glucose + drug treatment without glucose), simulating dietary intervention concurrent with chemotherapy;
(IV) Full Fasting (No glucose for the entire culture), representing an exclusively dietary-based fasting intervention;
(V) Fasting + High and drug (pre-conditioning without glucose + drug treatment with glucose), simulating chemotherapy with dietary intervention during the pre-treatment phase only;
(VI) Full Fasting + drug (pre-conditioning without glucose + drug treatment without glucose), representing chemotherapy with fasting both prior to and during cisplatin treatment.

The overarching aim was to investigate potential differences induced by these distinct therapeutic combinations. After treatments, the 2D Static, 3D Static, and 3D Dynamic models were analyzed for cellular morphology and viability. Microscopy analysis of the 2D models (Figure 3.9A) revealed a markedly reduced cell amount across all treatment

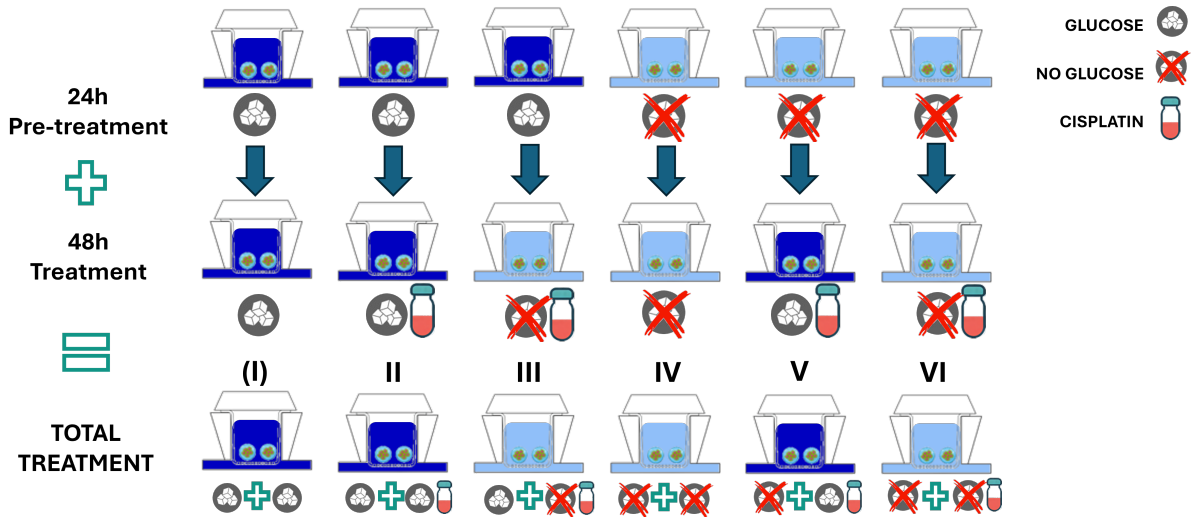

Figure 3.8: Chemotherapy-fasting experiment setup

groups compared to the control. Specifically, experimental groups (II) and (V) exhibited reduced proliferation, with cells appearing attached and elongated. In group (III), a greater number of dead and detached cells was observed. A similar condition was noted in group (VI), although the remaining live cells exhibited a more elongated morphology. The fasting-only group (IV) also showed numerous dead and detached cells. Characterization of cell viability through Live & Dead assay provided results that were partially consistent with microscopic observations. A marked decrease in live cells compared to the control group was evident across all experimental conditions. Notably, groups (III), (V), and (VI) displayed an increased presence of dead cells, as indicated by red fluorescence (fig. 3.9). Among these, the Full Fasting group (VI) demonstrated the highest distribution of dead cells, accompanied by a reduction in cell spreading, as evidenced by the rounded and less extended morphology of the live cells. In the 2D Static model, the qualitative findings from the Live & Dead assay were in good agreement with the semi-quantitative viability outcomes obtained from the AlamarBlue assay. As depicted in Figure 3.9C, all experimental groups experienced a reduction in viability of at least 20% compared to the control, with the Full Fasting group (IV) demonstrating the most significant decline.

Fluorescence images from the Live & Dead assay of 3D samples (Figure 3.9B) exhibited minimal qualitative differences between experimental groups. Specifically, the 3D Static models showed a consistent distribution of live cells across all groups, with a low numbers of dead cells. A similar pattern was noted in the 3D dynamic model, although groups (II), (III), and (V) displayed a slight increase in dead cells. Particularly in group (VI), a localized region with a higher concentration of dead cells was more prominent.

In the 3D Static model, the viability percentages reflected the qualitative fluorescence

images, with no statistically significant difference between experimental groups (Figure 3.9D). However, a different scenario emerged for the 3D Dynamic cultures (Figure 3.9E). where significant differences were observed in several treatment groups compared to the control. Here, several treatment groups showed significant reductions in cell viability compared to the control, with all cisplatin-treated groups demonstrating a reduction in viability exceeding 50%, in comparison with control. Interestingly, while the Full Fasting + Drug treatment group displayed a less pronounced reduction in viability compared to the other drug treatments, in contrast with the apparent increase in cell death observed in the Live & Dead assay images (Figure 3.9B). This suggests a possible discrepancy between metabolic activity and cell death metrics that warrants further investigation.

The findings of this experiment highlight a clear distinction in cellular responses between the different models and treatments. In the 2D models, cells treated with cisplatin, fasting, or a combination of both exhibited significant negative effects. These were evident both qualitatively—through changes in cell morphology and distribution of live and dead cells—and semi-quantitatively, as reflected by viability assays. Interestingly, fasting alone seemed to exert slightly stronger effects than the combination of fasting and cisplatin, which is somewhat unexpected but may suggest an adaptive metabolic response in the absence of nutrients.

The results from the 3D static tumor models showed only limited evidence of drug efficacy, with viability percentages not reaching statistical significance. However, in the 3D dynamic models, the effect of the drug treatment was markedly more pronounced, emphasizing the importance of fluid flow in accurately replicating *in vivo* conditions. This dynamic environment, which mimics capillary circulation and systemic drug transport, plays a crucial role in drug delivery and tumor regression, as supported by various studies in the literature. The MIVO® tissue culture device was instrumental in creating these fluid-dynamic conditions, which more closely resemble *in vivo* tumor tissue perfusion and drug distribution. In a recent study, this device was used to test drug efficacy of cisplatin in 3D ovarian cancer model and results were compared with animal data [108]. Authors demonstrated that the device accelerated the tumor regression curve *in vitro*, achieving drug efficacy results comparable to those seen *in vivo* but in a shorter time frame (1 week *in vitro* compared to 5 weeks *in vivo*). This difference is attributed to variations in drug clearance and distribution in static versus dynamic conditions, highlighting the potential of dynamic 3D models as a more reliable platform for preclinical drug efficacy testing. These findings align with previous research demonstrating that flow conditions enhance drug delivery and treatment outcomes in 3D cultures [109, 110].

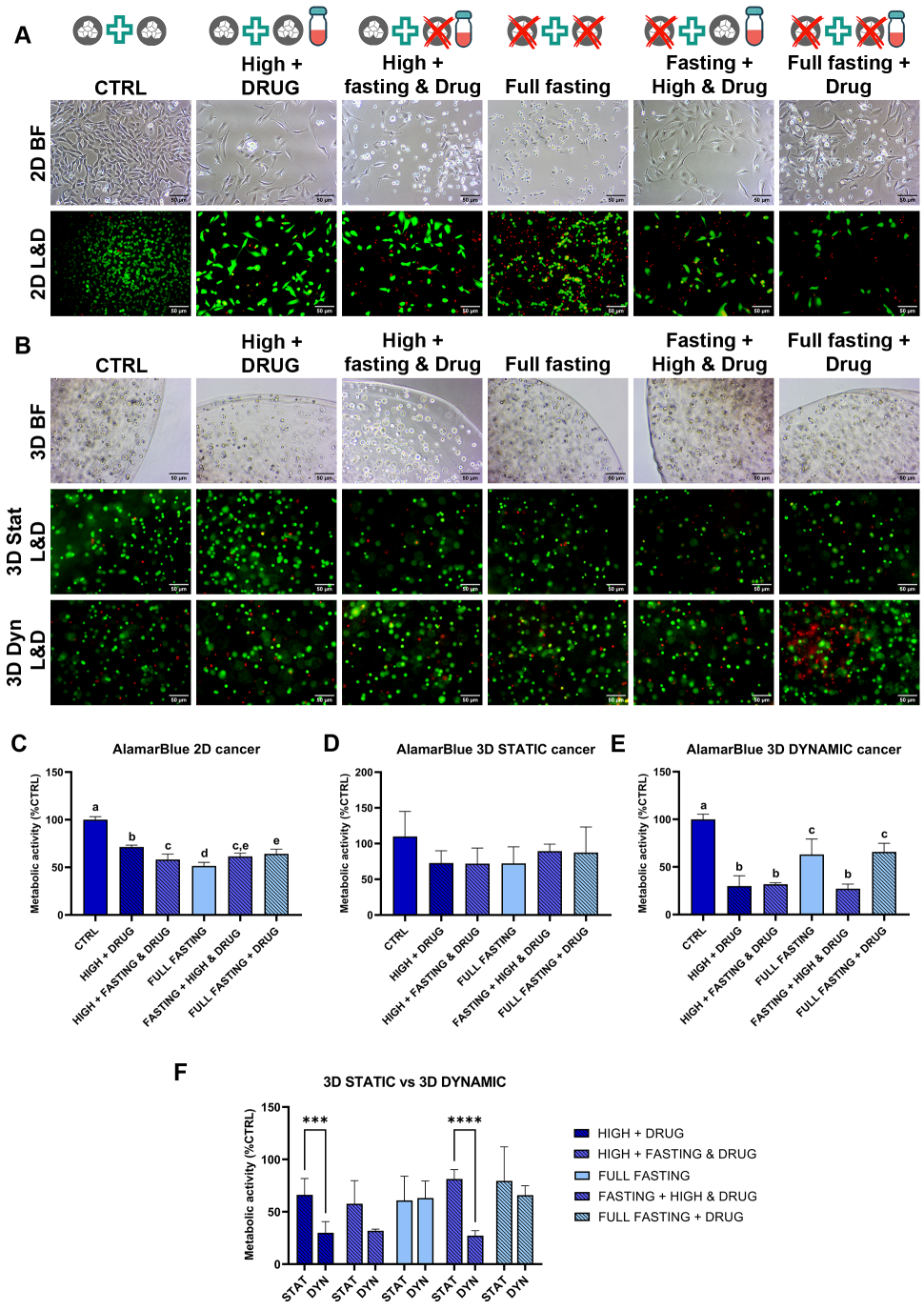

Figure 3.9: Effects of different fasting adjuvating chemotherapy treatment strategies on tumor models. Representative images of MDA-MB-231 cancer cells and Live & Dead staining both in 2D (A) and 3D (B) condition under different fasting and drug treatment. Scale bar: 50 µm. Cells viability by AlamarBlue assay in 2D (C), 3D static (D) and 3D dynamic (E) conditions. Semi-quantitative data are reported as mean ± SD and expressed as percentage of Control (High CTRL). (F) Comparison of cell viability data between 3D static and 3D dynamic culture conditions. Values with shared letters are not significantly different ($P > 0.05$) according with two-way ANOVA. N=2.

Finally, dynamic culture conditions significantly influenced the distribution and recirculation of nutrients and biomolecules within the 3D tumor microenvironment, leading to enhanced cellular access to these critical resources [111–113]. In the fasting-only group (IV), the viability percentages were comparable to the control, which may be explained by the fluid flow's ability to more effectively distribute even small residual amounts of glucose throughout the matrix, allowing improved cell survival under nutrient-limited conditions. Additionally, dynamic flow conditions might have triggered a metabolic shift, increasing the metabolic plasticity of cancer cells and enabling them to better adapt to challenging conditions, such as glucose deprivation [39, 114]. This metabolic adaptation also likely explains the results in the cisplatin and fasting group (VI). In this case, fasting may have induced protective autophagy or other bioactive changes that reduced cisplatin efficacy. Under nutrient-deprived and hypoxic conditions, cancer cells tend to slow their proliferation and enhance their DNA repair mechanisms, decreasing their sensitivity to chemotherapy. This is consistent with literature suggesting that cancer cells can become more resilient under stress through such mechanisms [115, 116].

Overall, this experiment underscores the value of using 3D dynamic models, particularly the MIVO® single-flow organ-on-chip device, which closely mimics the tumor microenvironment. While the fasting-drug strategies examined in some groups (III and V) did not result in significant differences compared to chemotherapy alone (II), the continuous fasting combined with cisplatin (VI) presented outcomes that highlight the complexity of cellular responses under glucose deprivation and demand further investigation into potential therapeutic synergies.

In conclusion, the study highlights the potential for fasting and glucose deprivation to induce protective mechanisms in cancer cells, such as autophagy and metabolic adaptation, which could reduce the efficacy of chemotherapeutic agents like cisplatin. These findings underscore the complexity of cancer cell responses to metabolic stress and the possibility of fostering treatment resistance through certain fasting strategies. Thus, it is critical to carefully balance these interventions in therapeutic settings, ensuring that they do not inadvertently enhance tumor resilience while attempting to target cancer metabolism. Further research is essential to optimize fasting-drug combinations to maximize efficacy while minimizing the risk of inducing resistance.

3.6. Healthy tissue models exhibit superior resilience compared to tumor models under Fasting and Chemotherapy

To obtain data that more closely reflects *in vivo* physiological conditions, it is essential to evaluate the response of healthy tissues to the same treatment protocols applied to pathological models. This approach provides a critical reference point for comparison, allowing for a more accurate estimation of the therapy's potential effects on a hypothetical clinical patient. By replicating the experimental conditions previously tested on pathological tissues, we aimed to assess how healthy tissue responds to treatments designed for diseased contexts, thereby contributing to a deeper understanding of the differential impacts of the therapy on pathological versus non-pathological environments.

Human dermal fibroblasts (HDFs) were used to create healthy tissue models, including 2D static, 3D static, and 3D dynamic cultures. These models were subjected to the same treatments previously applied to the TNBC models, resulting in a set of experimental groups that mirrored the tumor models.

From the morphological analysis, both visible light microscopy and Live & Dead assay (Figure 3.10) revealed that in the 2D static model, the ells exhibit near-optimal conditions across all experimental groups. Specifically, all groups showed good adhesion and elongation, with no signs of rounded or detached cells, which would indicate cellular distress. Furthermore, qualitatively less cells were observed in the experimental groups (II), (III), and (V), suggesting a slight decrease in cell proliferation.

The preliminary qualitative observations of the 2D samples were confirmed by the semi-quantitative results from the AlamarBlue viability assay. As shown in Figure 3.10C, all experimental groups exhibited cell viability greater than 50% compared to the control. However, the experimental groups treated with cisplatin showed a decrease in viability, with group (III) exhibiting a more significant reduction than the other treatments. The Full Fasting treatment (IV), in terms of metabolic activity, showed a response comparable to the control (I).

In the 3D models, as seen in previous experiments, morphological analysis did not reveal qualitative differences in the visible light or fluorescence images. Cells within the 3D matrix appear to have a typically round shape, as shown in Figure 3.10B. Fluorescence images obtained from the Live & Dead assay, in both 3D Static and 3D Dynamic models, qualitatively demonstrate a good distribution of live cells, distinguishable by their

green fluorescence, as shown in Figure 3.10B. Dead cells, visible in red, appeared more concentrated in the experimental groups (III) and (IV) of the static cultures. Conversely, the dynamic cultures did not exhibit any significant qualitative differences in viability between the experimental groups.

The semi-quantitative viability analysis conducted on the 3D models confirms the qualitative observations from the Live & Dead assay. As shown in Figure 3.10D, the experimental groups (II), (V), and (VI) displayed high viability percentages compared to the control. However, a slight decrease in viability was observed in groups (III) and (IV). In the 3D dynamic cultures, the metabolic activity assessments from the AlamarBlue assay appear to confirm a generally positive viability condition across all experimental groups, as shown in Figure 3.10E. Moreover, the differences observed between experimental groups in the 3D Static model seem to be less pronounced.

From the analysis of the results, it can be concluded that *in vitro* models of healthy tissue, regardless of their complexity, show minimal responses to treatments involving fasting and/or chemotherapy drugs. Specifically, cell viability remains positive in most cases, and is often comparable to the control group. In static 2D cultures, slight differences in viability are observed, but these are not evident in the more biomimetic dynamic culture models. In dynamic models, which more closely replicate the *in vivo* environment with continuous nutrient flow and active tissue perfusion, the cell response might be modulated by the presence of nutrient gradients, further emphasizing the role of the physiological environment in determining the cellular outcome. These findings underscore the need for careful consideration when translating fasting or metabolic interventions into clinical practice, particularly in cancer therapies, where the balance between enhancing drug efficacy and minimizing harm to normal tissues is critical. Overall, the comparison between the TNBC models and healthy tissue (HDFas) revealed significant differences, particularly in response to fasting and chemotherapy treatments. The analysis of metabolic activity assays in the respective *in vitro* models clearly indicates discriminating outcomes. As shown in Figure 3.10F, a marked difference in cell viability was observed across the experimental groups, with healthy tissue samples showing less negative effects compared to their tumor counterparts. Notably, after the Full Fasting (IV) treatment, the viability of the healthy tissue model (HDFas) was approximately double that observed in the TNBC model (MDA-MB-231). While positive differences were also noted in the drug-treated groups, the gap was less pronounced than in the Full Fasting group.

In the 3D Static model Figure 3.10G), with the exception of group (II), there were no significant differences between healthy and tumor models, reinforcing the idea that the response in these simpler systems might not fully capture the complexities of cancer-

ous tissues. However, the situation differed in the 3D Dynamic models (Figure 3.10H). Consistent with observations in 2D cultures, drug-treated groups (II), (III), (V), and (VI) displayed lower viability in the tumor model compared to the corresponding healthy model. The negative effects induced by treatment in the tumor models were significantly more pronounced than in healthy tissue. This underscores the sensitivity of cancer cells to chemotherapy treatments, with healthy cells showing a more favorable response under similar conditions. Interestingly, the Full Fasting (IV) group did not show significant differences between the healthy and tumor models. This suggests that, under fasting conditions, both cell types may adapt similarly, likely due to the metabolic changes induced by nutrient deprivation, which can trigger cellular protective mechanisms such as autophagy.

The observed results underscore the differential sensitivity between cancerous and healthy tissues to metabolic stress and chemotherapy. Fasting as a therapeutic strategy has gained attention due to its potential to sensitize tumor cells while preserving healthy tissue [112]. In cancer cells, fasting can induce autophagy and metabolic stress, which may enhance the efficacy of chemotherapy agents like cisplatin. However, the fact that healthy cells, particularly fibroblasts, seem to fare better in response to fasting than tumor cells suggests that a well-balanced fasting protocol may mitigate detrimental effects on normal tissues while still exploiting the vulnerabilities of cancer cells.

In dynamic 3D models, which better replicate *in vivo*-like conditions, the sensitivity to treatment was more pronounced, particularly in tumor cells. This further emphasizes the importance of using more biomimetic models to assess therapeutic strategies, as they provide a more accurate representation of the tumor microenvironment and drug delivery dynamics [117, 118]. Additionally, dynamic flow can influence nutrient and drug distribution, which might explain the observed effects in the Full Fasting group, where no significant difference was noted between healthy and cancerous tissues. This suggests that the metabolic adjustments triggered by fasting may create an adaptive environment where both cell types manage stress similarly under these specific conditions.

These findings are in line with studies suggesting that fasting and metabolic interventions must be carefully balanced to avoid inducing resistance mechanisms in cancer cells or excessive damage to healthy tissue [119–121]. Further research is necessary to explore the long-term effects and optimal conditions for combining fasting with chemotherapy to maximize therapeutic efficacy while minimizing side effects.

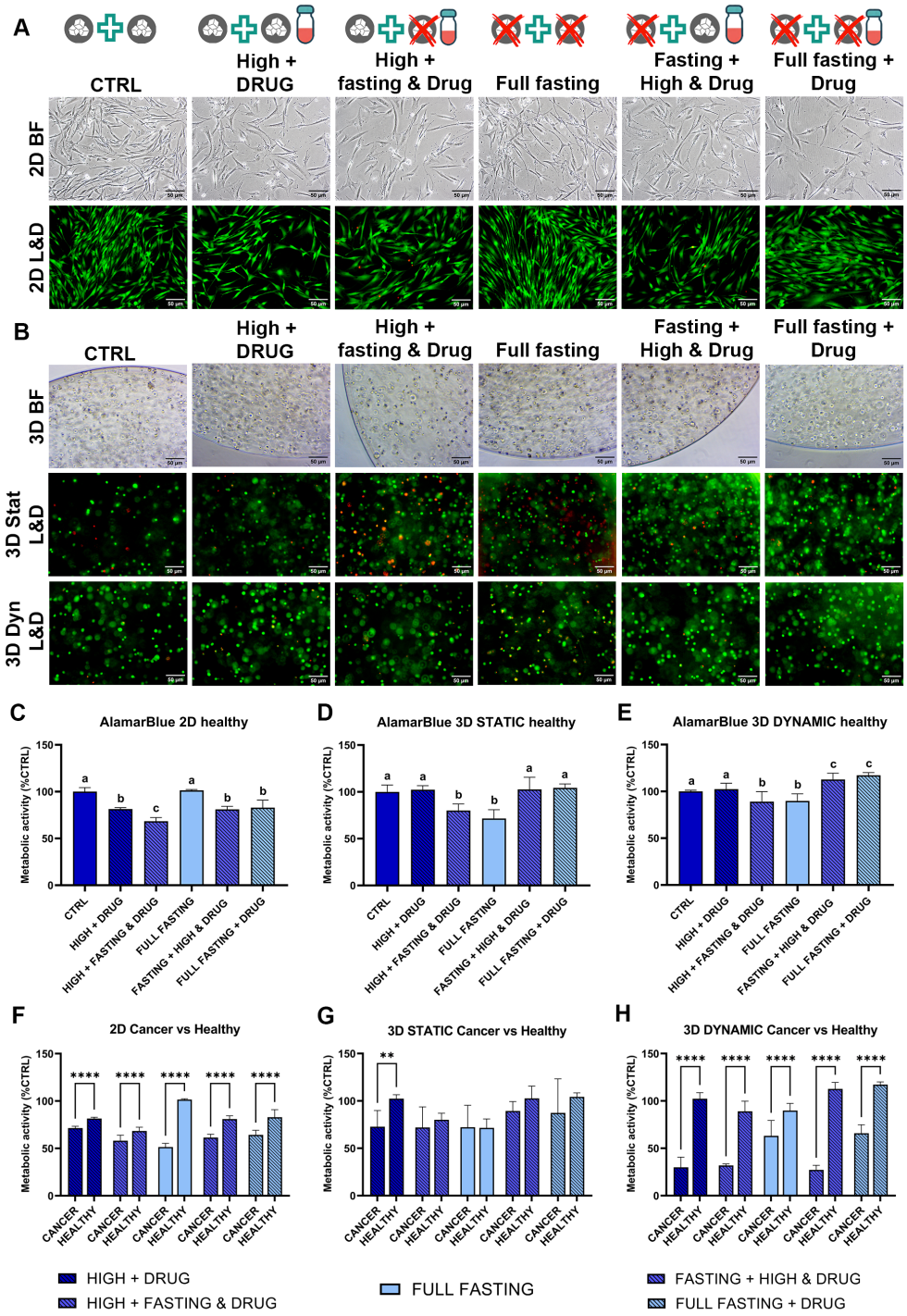

Figure 3.10: Effects of different fasting adjuvating chemotherapy treatment strategies on healthy models. Representative images of HDFas cells and Live & Dead staining both in 2D (A) and 3D (B) condition under different fasting and drug treatment. Scale bar: 50 µm. Cells viability by AlamarBlue assay in 2D (C), 3D static (D) and 3D dynamic (E) conditions. Semi-quantitative data are reported as mean ± SD and expressed as percentage of Control (High CTRL). Comparison of cell viability data between cancer and healthy cells in 2D (F), 3D static (G) and 3D dynamic (H) culture conditions. Values with shared letters are not significantly different ($P > 0.05$) according with two-way ANOVA. N=2.

4 | Conclusions and future developments

This study highlights the significant advancements made in understanding the effects of glucose restriction and chemotherapy on TNBC through the development of a novel 3D *in vitro* model integrated into an organ-on-chip platform. Recent clinical trials have also explored the influence of dietary interventions, including glucose restriction, on cancer progression and treatment efficacy. These trials have shown promising results, particularly when dietary changes are combined with conventional therapies, further supporting the relevance of studying the impact of dietary interventions in cancer treatment. The findings emphasize the importance of utilizing 3D models, particularly in dynamic culture conditions, to more accurately replicate the *in vivo* tumor microenvironment. This approach not only enhances the relevance of drug testing but also provides more meaningful insights into the complex interactions between cancer cells and their microenvironment.

While glucose restriction significantly reduced tumor cell viability in 2D cultures, a pronounced difference was observed in the 3D models. Specifically, the 3D static cultures showed minimal response to glucose deprivation and chemotherapy treatments, indicating the limitations of static 3D models in simulating the true tumor microenvironment. In contrast, 3D dynamic cultures demonstrated a significant improvement in drug diffusion and chemotherapy efficacy, closely resembling the *in vivo* conditions of fluid dynamics and systemic drug delivery. This highlights the critical role of dynamic flow in 3D models, which allows for better representation of tumor behavior, including nutrient and drug distribution, and provides a more accurate platform for testing therapeutic strategies.

The dynamic culture conditions, as seen in the organ-on-chip platform, enhanced drug efficacy by mimicking the blood circulation's impact on drug transport, allowing a more realistic assessment of how tumor cells interact with therapeutic agents. These results emphasize that when studying cancer biology or testing therapeutic strategies, it is essential to incorporate dynamic flow into 3D models. This dynamic environment facilitates proper cell-to-cell interactions and nutrient exchange, which are often absent in static

cultures, leading to more reliable predictions of drug response.

The interaction between fasting and chemotherapy in this model also provided intriguing insights, particularly regarding cell proliferation and hypoxia. While combined fasting and chemotherapy resulted in decreased tumor viability, cells remained proliferative and hypoxic, suggesting the need for further exploration of these combined strategies. This finding underscores the complexity of cancer cell response to metabolic stressors and therapeutic interventions, warranting additional studies to refine our understanding of their synergistic effects. The presence of both Ki67 and HIF-1α in the tumor models suggests that despite reduced viability, tumor cells continue to exhibit aggressive behavior under fasting conditions, pointing to the potential for resistance mechanisms such as enhanced DNA repair and metabolic plasticity.

Overall, the organ-on-chip platform demonstrated its utility as a predictive model for studying tumor biology, drug efficacy, and the interplay between fasting and chemotherapy. The ability to recreate controlled 3D microenvironments and dynamic flow conditions makes this system an invaluable tool for preclinical drug testing and understanding tumor progression. Additionally, its potential applications extend beyond cancer research, offering promising avenues for regenerative medicine and tissue engineering, where similar principles of tissue perfusion and cellular behavior under dynamic conditions are critical.

Future research should focus on enhancing the accuracy and applicability of the tumor model. A key area is improving the biomimicry of the tumor microenvironment by integrating a more heterogeneous cell population (fibroblast CAFs, immune cells TAMs), while also employing diverse biomaterials to increase TME complexity. It would also be valuable to further investigate the combined effects of dietary modifications and chemotherapy, particularly to elucidate cellular responses, including the mechanisms of induced cellular death and the potential role of autophagy. Moreover, exploring the integration of these strategies with immunotherapies could offer new insights into enhancing therapeutic efficacy.

In conclusion, the combination of 3D dynamic models and organ-on-chip technology represents a leap forward in the study of cancer biology and treatment. However, further investigations are needed to better understand the long-term effects of fasting and chemotherapy on tumor cell metabolism and to optimize strategies that minimize resistance and maximize therapeutic efficacy.

Bibliography

[1] Joel S. Brown, Sarah R. Amend, Robert H. Austin, Robert A. Gatenby, Emma U. Hammarlund, and Kenneth J. Pienta. Updating the definition of cancer. *Molecular Cancer Research*, 21(11):1142–1147, July 2023. ISSN 1557-3125. doi: 10.1158/1541-7786.mcr-23-0411. URL http://dx.doi.org/10.1158/1541-7786.MCR-23-0411.

[2] Camilla Mattiuzzi and Giuseppe Lippi. Current cancer epidemiology. *Journal of Epidemiology and Global Health*, 9(4):217, 2019. ISSN 2210-6014. doi: 10.2991/jegh.k.191008.001. URL http://dx.doi.org/10.2991/jegh.k.191008.001.

[3] Nadia Harbeck, Frédérique Penault-Llorca, Javier Cortes, Michael Gnant, Nehmat Houssami, Philip Poortmans, Kathryn Ruddy, Janice Tsang, and Fatima Cardoso. Breast cancer. *Nature Reviews Disease Primers*, 5(1), September 2019. ISSN 2056-676X. doi: 10.1038/s41572-019-0111-2. URL http://dx.doi.org/10.1038/s41572-019-0111-2.

[4] M. De Laurentiis, D. Cianniello, R. Caputo, B Stanzione, G. Arpino, S. Cinieri, V. Lorusso, and S. De Placido. Treatment of triple negative breast cancer (tnbc): current options and future perspectives. *Cancer Treatment Reviews*, 36:S80–S86, November 2010. ISSN 0305-7372. doi: 10.1016/s0305-7372(10)70025-6. URL http://dx.doi.org/10.1016/S0305-7372(10)70025-6.

[5] Li Yin, Jiang-Jie Duan, Xiu-Wu Bian, and Shi-cang Yu. Triple-negative breast cancer molecular subtyping and treatment progress. *Breast Cancer Research*, 22 (1), June 2020. ISSN 1465-542X. doi: 10.1186/s13058-020-01296-5. URL http://dx.doi.org/10.1186/s13058-020-01296-5.

[6] Yang Chang-Qing, Liu Jie, Zhao Shi-Qi, Zhu Kun, Gong Zi-Qian, Xu Ran, Lu Hui-Meng, Zhou Ren-Bin, Zhao Gang, Yin Da-Chuan, and Zhang Chen-Yan. Recent treatment progress of triple negative breast cancer. *Progress in Biophysics and Molecular Biology*, 151:40–53, March 2020. ISSN 0079-6107. doi: 10.1016/j.

pbiomolbio.2019.11.007. URL http://dx.doi.org/10.1016/j.pbiomolbio.2019.11.007.

[7] Paola Zagami and Lisa Anne Carey. Triple negative breast cancer: Pitfalls and progress. *npj Breast Cancer*, 8(1), August 2022. ISSN 2374-4677. doi: 10.1038/s41523-022-00468-0. URL http://dx.doi.org/10.1038/s41523-022-00468-0.

[8] Yun Li, Huajun Zhang, Yulia Merkher, Lin Chen, Na Liu, Sergey Leonov, and Yongheng Chen. Recent advances in therapeutic strategies for triple-negative breast cancer. *Journal of Hematology & Oncology*, 15(1), August 2022. ISSN 1756-8722. doi: 10.1186/s13045-022-01341-0. URL http://dx.doi.org/10.1186/s13045-022-01341-0.

[9] Allison N. Lau and Matthew G. Vander Heiden. Metabolism in the tumor microenvironment. *Annual Review of Cancer Biology*, 4(1):17–40, March 2020. ISSN 2472-3428. doi: 10.1146/annurev-cancerbio-030419-033333. URL http://dx.doi.org/10.1146/annurev-cancerbio-030419-033333.

[10] Pengfei Lu, Valerie M. Weaver, and Zena Werb. The extracellular matrix: A dynamic niche in cancer progression. *Journal of Cell Biology*, 196(4):395–406, February 2012. ISSN 0021-9525. doi: 10.1083/jcb.201102147. URL http://dx.doi.org/10.1083/jcb.201102147.

[11] Miguel Reina-Campos, Jorge Moscat, and Maria Diaz-Meco. Metabolism shapes the tumor microenvironment. *Current Opinion in Cell Biology*, 48:47–53, October 2017. ISSN 0955-0674. doi: 10.1016/j.ceb.2017.05.006. URL http://dx.doi.org/10.1016/j.ceb.2017.05.006.

[12] Juan F. Linares, Thekla Cordes, Angeles Duran, Miguel Reina-Campos, Tania Valencia, Christopher S. Ahn, Elias A. Castilla, Jorge Moscat, Christian M. Metallo, and Maria T. Diaz-Meco. Atf4-induced metabolic reprograming is a synthetic vulnerability of the p62-deficient tumor stroma. *Cell Metabolism*, 26(6):817–829.e6, December 2017. ISSN 1550-4131. doi: 10.1016/j.cmet.2017.09.001. URL http://dx.doi.org/10.1016/j.cmet.2017.09.001.

[13] Cristovão M. Sousa, Douglas E. Biancur, Xiaoxu Wang, Christopher J. Halbrook, Mara H. Sherman, Li Zhang, Daniel Kremer, Rosa F. Hwang, Agnes K. Witkiewicz, Haoqiang Ying, John M. Asara, Ronald M. Evans, Lewis C. Cantley, Costas A. Lyssiotis, and Alec C. Kimmelman. Pancreatic stellate cells support tumour metabolism through autophagic alanine secretion. *Nature*, 536(7617):

479–483, August 2016. ISSN 1476-4687. doi: 10.1038/nature19084. URL http://dx.doi.org/10.1038/nature19084.

[14] Tania Valencia, Ji Young Kim, Shadi Abu-Baker, Jorge Moscat-Pardos, Christopher S. Ahn, Miguel Reina-Campos, Angeles Duran, Elias A. Castilla, Christian M. Metallo, Maria T. Diaz-Meco, and Jorge Moscat. Metabolic reprogramming of stromal fibroblasts through p62-mtorc1 signaling promotes inflammation and tumorigenesis. *Cancer Cell*, 26(1):121–135, July 2014. ISSN 1535-6108. doi: 10.1016/j.ccr.2014.05.004. URL http://dx.doi.org/10.1016/j.ccr.2014.05.004.

[15] Chih-Hao Chang, Jing Qiu, David O'Sullivan, Michael D. Buck, Takuro Noguchi, Jonathan D. Curtis, Qiongyu Chen, Mariel Gindin, Matthew M. Gubin, Gerritje J.W. van der Windt, Elena Tonc, Robert D. Schreiber, Edward J. Pearce, and Erika L. Pearce. Metabolic competition in the tumor microenvironment is a driver of cancer progression. *Cell*, 162(6):1229–1241, September 2015. ISSN 0092-8674. doi: 10.1016/j.cell.2015.08.016. URL http://dx.doi.org/10.1016/j.cell.2015.08.016.

[16] Shiqi Nong, Xiaoyue Han, Yu Xiang, Yuran Qian, Yuhao Wei, Tingyue Zhang, Keyue Tian, Kai Shen, Jing Yang, and Xuelei Ma. Metabolic reprogramming in cancer: Mechanisms and therapeutics. *MedComm*, 4(2), March 2023. ISSN 2688-2663. doi: 10.1002/mco2.218. URL http://dx.doi.org/10.1002/mco2.218.

[17] Otto Warburg, Franz Wind, and Erwin Negelein. The metabolism of tumors in the body. *Journal of General Physiology*, 8(6):519–530, March 1927. ISSN 0022-1295. doi: 10.1085/jgp.8.6.519. URL http://dx.doi.org/10.1085/jgp.8.6.519.

[18] Karol Bukowski, Mateusz Kciuk, and Renata Kontek. Mechanisms of multidrug resistance in cancer chemotherapy. *International Journal of Molecular Sciences*, 21(9):3233, May 2020. ISSN 1422-0067. doi: 10.3390/ijms21093233. URL http://dx.doi.org/10.3390/ijms21093233.

[19] Elena Dickens and Samreen Ahmed. Principles of cancer treatment by chemotherapy. *Surgery (Oxford)*, 36(3):134–138, March 2018. ISSN 0263-9319. doi: 10.1016/j.mpsur.2017.12.002. URL http://dx.doi.org/10.1016/j.mpsur.2017.12.002.

[20] Elisabeth Åvall Lundqvist, Keiichi Fujiwara, and Muhieddine Seoud. Principles of chemotherapy. *International Journal of Gynecology & Obstetrics*, 131(S2), September 2015. ISSN 1879-3479. doi: 10.1016/j.ijgo.2015.06.011. URL http://dx.doi.org/10.1016/j.ijgo.2015.06.011.

[21] J. Kashifa Fathima, V. Lavanya, Shazia Jamal, and Neesar Ahmed. The effectiveness

of various chemotherapeutic agents in cancer treatment. *Current Pharmacology Reports*, 8(4):236–252, May 2022. ISSN 2198-641X. doi: 10.1007/s40495-022-00289-6. URL http://dx.doi.org/10.1007/s40495-022-00289-6.

[22] Asmita Yadav, Sakshi Singh, Harmik Sohi, and Shweta Dang. Advances in delivery of chemotherapeutic agents for cancer treatment. *AAPS PharmSciTech*, 23 (1), December 2021. ISSN 1530-9932. doi: 10.1208/s12249-021-02174-9. URL http://dx.doi.org/10.1208/s12249-021-02174-9.

[23] Sumit Ghosh. Cisplatin: The first metal based anticancer drug. *Bioorganic Chemistry*, 88:102925, July 2019. ISSN 0045-2068. doi: 10.1016/j.bioorg.2019.102925. URL http://dx.doi.org/10.1016/j.bioorg.2019.102925.

[24] Tomaz Makovec. Cisplatin and beyond: molecular mechanisms of action and drug resistance development in cancer chemotherapy. *Radiology and Oncology*, 53(2): 148–158, March 2019. ISSN 1581-3207. doi: 10.2478/raon-2019-0018. URL http://dx.doi.org/10.2478/raon-2019-0018.

[25] Barnett Rosenberg, Loretta Van Camp, Eugene B. Grimley, and Andrew J. Thomson. The inhibition of growth or cell division in escherichia coli by different ionic species of platinum(iv) complexes. *Journal of Biological Chemistry*, 242(6): 1347–1352, March 1967. ISSN 0021-9258. doi: 10.1016/s0021-9258(18)96186-7. URL http://dx.doi.org/10.1016/s0021-9258(18)96186-7.

[26] Anže Martinčič, Maja Cemazar, Gregor Sersa, Viljem Kovač, Radmila Milačič, and Janez Ščančar. A novel method for speciation of pt in human serum incubated with cisplatin, oxaliplatin and carboplatin by conjoint liquid chromatography on monolithic disks with uv and icp-ms detection. *Talanta*, 116:141–148, November 2013. ISSN 0039-9140. doi: 10.1016/j.talanta.2013.05.016. URL http://dx.doi.org/10.1016/j.talanta.2013.05.016.

[27] Minerva, Amrita Bhat, Sonali Verma, Gresh Chander, Rajeshwer Singh Jamwal, Bhawani Sharma, Audesh Bhat, Taruna Katyal, Rakesh Kumar, and Ruchi Shah. Cisplatin-based combination therapy for cancer. *Journal of Cancer Research and Therapeutics*, 19(3):530–536, April 2023. ISSN 1998-4138. doi: 10.4103/jcrt.jcrt_792_22. URL http://dx.doi.org/10.4103/jcrt.jcrt_792_22.

[28] Sofia RE Mason, Melina L Willson, Sam J Egger, Jane Beith, Rachel F Dear, and Annabel Goodwin. Platinum-based chemotherapy for early triple-negative breast cancer. *Cochrane Database of Systematic Reviews*, 2023(9), September 2023. ISSN

1465-1858. doi: 10.1002/14651858.cd014805.pub2. URL http://dx.doi.org/10.1002/14651858.CD014805.pub2.

[29] Kapila Ratnam and Jennifer A. Low. Current development of clinical inhibitors of poly(adp-ribose) polymerase in oncology. *Clinical Cancer Research*, 13(5): 1383–1388, March 2007. ISSN 1557-3265. doi: 10.1158/1078-0432.ccr-06-2260. URL http://dx.doi.org/10.1158/1078-0432.CCR-06-2260.

[30] Roberto A Leon-Ferre and Matthew P Goetz. Advances in systemic therapies for triple negative breast cancer. *BMJ*, page e071674, May 2023. ISSN 1756-1833. doi: 10.1136/bmj-2022-071674. URL http://dx.doi.org/10.1136/bmj-2022-071674.

[31] L Galluzzi, L Senovilla, I Vitale, J Michels, I Martins, O Kepp, M Castedo, and G Kroemer. Molecular mechanisms of cisplatin resistance. *Oncogene*, 31(15): 1869–1883, September 2011. ISSN 1476-5594. doi: 10.1038/onc.2011.384. URL http://dx.doi.org/10.1038/onc.2011.384.

[32] Helen H. W. Chen and Macus Tien Kuo. Role of glutathione in the regulation of cisplatin resistance in cancer chemotherapy. *Metal-Based Drugs*, 2010: 1–7, September 2010. ISSN 1687-5486. doi: 10.1155/2010/430939. URL http://dx.doi.org/10.1155/2010/430939.

[33] Alex D. Lewis, John D. Hayes, and C. Roland Wolf. Glutathione and glutathione-dependent enzymes in ovarian adenocarcinoma cell lines derived from a patient before and after the onset of drug resistance: intrinsic differences and cell cycle effects. *Carcinogenesis*, 9(7):1283–1287, 1988. ISSN 1460-2180. doi: 10.1093/carcin/9.7.1283. URL http://dx.doi.org/10.1093/carcin/9.7.1283.

[34] Ji Hyun Park, Jin-Hee Ahn, and Sung-Bae Kim. How shall we treat early triple-negative breast cancer (tnbc): from the current standard to upcoming immuno-molecular strategies. *ESMO Open*, 3:e000357, 2018. ISSN 2059-7029. doi: 10.1136/esmoopen-2018-000357. URL http://dx.doi.org/10.1136/esmoopen-2018-000357.

[35] Shree Bose, Annamarie E. Allen, and Jason W. Locasale. The molecular link from diet to cancer cell metabolism. *Molecular Cell*, 78(6):1034–1044, June 2020. ISSN 1097-2765. doi: 10.1016/j.molcel.2020.05.018. URL http://dx.doi.org/10.1016/j.molcel.2020.05.018.

[36] Junfeng Bi, Sudhir Chowdhry, Sihan Wu, Wenjing Zhang, Kenta Masui, and Paul S. Mischel. Altered cellular metabolism in gliomas — an emerging landscape of actionable co-dependency targets. *Nature Reviews Cancer*, 20(1):57–70,

December 2019. ISSN 1474-1768. doi: 10.1038/s41568-019-0226-5. URL http://dx.doi.org/10.1038/s41568-019-0226-5.

[37] Matthew G. Vander Heiden and Ralph J. DeBerardinis. Understanding the intersections between metabolism and cancer biology. *Cell*, 168(4):657–669, February 2017. ISSN 0092-8674. doi: 10.1016/j.cell.2016.12.039. URL http://dx.doi.org/10.1016/j.cell.2016.12.039.

[38] Adam J. Wolpaw and Chi V. Dang. Exploiting metabolic vulnerabilities of cancer with precision and accuracy. *Trends in Cell Biology*, 28(3):201–212, March 2018. ISSN 0962-8924. doi: 10.1016/j.tcb.2017.11.006. URL http://dx.doi.org/10.1016/j.tcb.2017.11.006.

[39] Wilhelm Palm and Craig B. Thompson. Nutrient acquisition strategies of mammalian cells. *Nature*, 546(7657):234–242, June 2017. ISSN 1476-4687. doi: 10.1038/nature22379. URL http://dx.doi.org/10.1038/nature22379.

[40] Jiajun Zhu and Craig B. Thompson. Metabolic regulation of cell growth and proliferation. *Nature Reviews Molecular Cell Biology*, 20(7):436–450, April 2019. ISSN 1471-0080. doi: 10.1038/s41580-019-0123-5. URL http://dx.doi.org/10.1038/s41580-019-0123-5.

[41] Samantha J. Mentch, Mahya Mehrmohamadi, Lei Huang, Xiaojing Liu, Diwakar Gupta, Dwight Mattocks, Paola Gómez Padilla, Gene Ables, Marcas M. Bamman, Anna E. Thalacker-Mercer, Sailendra N. Nichenametla, and Jason W. Locasale. Histone methylation dynamics and gene regulation occur through the sensing of one-carbon metabolism. *Cell Metabolism*, 22(5):861–873, November 2015. ISSN 1550-4131. doi: 10.1016/j.cmet.2015.08.024. URL http://dx.doi.org/10.1016/j.cmet.2015.08.024.

[42] Otília Menyhárt and Balázs Győrffy. Dietary approaches for exploiting metabolic vulnerabilities in cancer. *Biochimica et Biophysica Acta (BBA) - Reviews on Cancer*, 1879(2):189062, March 2024. ISSN 0304-419X. doi: 10.1016/j.bbcan.2023.189062. URL http://dx.doi.org/10.1016/j.bbcan.2023.189062.

[43] Naama Kanarek, Boryana Petrova, and David M. Sabatini. Dietary modifications for enhanced cancer therapy. *Nature*, 579(7800):507–517, March 2020. ISSN 1476-4687. doi: 10.1038/s41586-020-2124-0. URL http://dx.doi.org/10.1038/s41586-020-2124-0.

[44] Lin Qian, Fan Zhang, Miao Yin, and Qunying Lei. Cancer metabolism and dietary interventions. *Cancer Biology & Medicine*, December 2021. ISSN 2095-3941.

doi: 10.20892/j.issn.2095-3941.2021.0461. URL http://dx.doi.org/10.20892/j.issn.2095-3941.2021.0461.

[45] Mengmeng Lv, Xingya Zhu, Hao Wang, Feng Wang, and Wenxian Guan. Roles of caloric restriction, ketogenic diet and intermittent fasting during initiation, progression and metastasis of cancer in animal models: A systematic review and meta-analysis. *PLoS ONE*, 9(12):e115147, December 2014. ISSN 1932-6203. doi: 10.1371/journal.pone.0115147. URL http://dx.doi.org/10.1371/journal.pone.0115147.

[46] Mehdi Sadeghian, Sepideh Rahmani, Saman Khalesi, and Ehsan Hejazi. A review of fasting effects on the response of cancer to chemotherapy. *Clinical Nutrition*, 40 (4):1669–1681, April 2021. ISSN 0261-5614. doi: 10.1016/j.clnu.2020.10.037. URL http://dx.doi.org/10.1016/j.clnu.2020.10.037.

[47] T N Seyfried, T M Sanderson, M M El-Abbadi, R McGowan, and P Mukherjee. Role of glucose and ketone bodies in the metabolic control of experimental brain cancer. *British Journal of Cancer*, 89(7):1375–1382, September 2003. ISSN 1532-1827. doi: 10.1038/sj.bjc.6601269. URL http://dx.doi.org/10.1038/sj.bjc.6601269.

[48] Lifeng Yang, Tara TeSlaa, Serina Ng, Michel Nofal, Lin Wang, Taijin Lan, Xianfeng Zeng, Alexis Cowan, Matthew McBride, Wenyun Lu, Shawn Davidson, Gaoyang Liang, Tae Gyu Oh, Michael Downes, Ronald Evans, Daniel Von Hoff, Jessie Yanxiang Guo, Haiyong Han, and Joshua D. Rabinowitz. Ketogenic diet and chemotherapy combine to disrupt pancreatic cancer metabolism and growth. *Med*, 3(2):119–136.e8, February 2022. ISSN 2666-6340. doi: 10.1016/j.medj.2021.12.008. URL http://dx.doi.org/10.1016/j.medj.2021.12.008.

[49] Xiuxiu Wang, Xiaoyu Liu, Zhenzhen Jia, Yilun Zhang, Shuo Wang, and Hongyan Zhang. Evaluation of the effects of different dietary patterns on breast cancer: Monitoring circulating tumor cells. *Foods*, 10(9):2223, September 2021. ISSN 2304-8158. doi: 10.3390/foods10092223. URL http://dx.doi.org/10.3390/foods10092223.

[50] N. Erickson, A. Boscheri, B. Linke, and J. Huebner. Systematic review: isocaloric ketogenic dietary regimes for cancer patients. *Medical Oncology*, 34(5), March 2017. ISSN 1559-131X. doi: 10.1007/s12032-017-0930-5. URL http://dx.doi.org/10.1007/s12032-017-0930-5.

[51] Rainer J. Klement, Nanina Brehm, and Reinhart A. Sweeney. Ketogenic diets in medical oncology: a systematic review with focus on clinical outcomes. *Medical*

Oncology, 37(2), January 2020. ISSN 1559-131X. doi: 10.1007/s12032-020-1337-2. URL http://dx.doi.org/10.1007/s12032-020-1337-2.

[52] NATALIE JANSEN and HARALD WALACH. The development of tumours under a ketogenic diet in association with the novel tumour marker tktl1: A case series in general practice. *Oncology Letters*, 11(1):584–592, November 2015. ISSN 1792-1082. doi: 10.3892/ol.2015.3923. URL http://dx.doi.org/10.3892/ol.2015.3923.

[53] Adeleh Khodabakhshi, Mohammad Esmaeil Akbari, Hamid Reza Mirzaei, Hassan Mehrad-Majd, Miriam Kalamian, and Sayed Hossein Davoodi. Feasibility, safety, and beneficial effects of mct-based ketogenic diet for breast cancer treatment: A randomized controlled trial study. *Nutrition and Cancer*, 72(4):627–634, September 2019. ISSN 1532-7914. doi: 10.1080/01635581.2019.1650942. URL http://dx.doi.org/10.1080/01635581.2019.1650942.

[54] Daniel W Belsky, Kim M Huffman, Carl F Pieper, Idan Shalev, and William E Kraus. Change in the rate of biological aging in response to caloric restriction: Calerie biobank analysis. *The Journals of Gerontology: Series A*, 73(1):4–10, May 2017. ISSN 1758-535X. doi: 10.1093/gerona/glx096. URL http://dx.doi.org/10.1093/gerona/glx096.

[55] James L. Dorling, Eric Ravussin, Leanne M. Redman, Manju Bhapkar, Kim M. Huffman, Susan B. Racette, Sai K. Das, John W. Apolzan, William E. Kraus, Christoph Höchsmann, and Corby K. Martin. Effect of 2 years of calorie restriction on liver biomarkers: results from the calerie phase 2 randomized controlled trial. *European Journal of Nutrition*, 60(3):1633–1643, August 2020. ISSN 1436-6215. doi: 10.1007/s00394-020-02361-7. URL http://dx.doi.org/10.1007/s00394-020-02361-7.

[56] Luigi Fontana, Linda Partridge, and Valter D. Longo. Extending healthy life span—from yeast to humans. *Science*, 328(5976):321–326, April 2010. ISSN 1095-9203. doi: 10.1126/science.1172539. URL http://dx.doi.org/10.1126/science.1172539.

[57] Julie A. Mattison, Ricki J. Colman, T. Mark Beasley, David B. Allison, Joseph W. Kemnitz, George S. Roth, Donald K. Ingram, Richard Weindruch, Rafael de Cabo, and Rozalyn M. Anderson. Caloric restriction improves health and survival of rhesus monkeys. *Nature Communications*, 8(1), January 2017. ISSN 2041-1723. doi: 10.1038/ncomms14063. URL http://dx.doi.org/10.1038/ncomms14063.

[58] Marcus D. Goncalves, Benjamin D. Hopkins, and Lewis C. Cantley. Phosphatidylinositol 3-kinase, growth disorders, and cancer. *New England Journal of Medicine*,

379(21):2052–2062, November 2018. ISSN 1533-4406. doi: 10.1056/nejmra1704560. URL http://dx.doi.org/10.1056/nejmra1704560.

[59] F. Antunes, G.J. Pereira, M.G. Jasiulionis, C. Bincoletto, and S.S. Smaili. Nutritional shortage augments cisplatin-effects on murine melanoma cells. *Chemico-Biological Interactions*, 281:89–97, February 2018. ISSN 0009-2797. doi: 10.1016/j.cbi.2017.12.027. URL http://dx.doi.org/10.1016/j.cbi.2017.12.027.

[60] Edward Henry Mathews, Michelle Helen Visagie, Albertus Abram Meyer, Anna Margaretha Joubert, and George Edward Mathews. In vitro quantification: Long-term effect of glucose deprivation on various cancer cell lines. *Nutrition*, 74:110748, June 2020. ISSN 0899-9007. doi: 10.1016/j.nut.2020.110748. URL http://dx.doi.org/10.1016/j.nut.2020.110748.

[61] Marios Anemoulis, Antonios Vlastos, Vasileios Kachtsidis, and Spyridon N. Karras. Intermittent fasting in breast cancer: A systematic review and critical update of available studies. *Nutrients*, 15(3):532, January 2023. ISSN 2072-6643. doi: 10.3390/nu15030532. URL http://dx.doi.org/10.3390/nu15030532.

[62] Sebastian Brandhorst, In Young Choi, Min Wei, Chia Wei Cheng, Sargis Sedrakyan, Gerardo Navarrete, Louis Dubeau, Li Peng Yap, Ryan Park, Manlio Vinciguerra, Stefano Di Biase, Hamed Mirzaei, Mario G. Mirisola, Patra Childress, Lingyun Ji, Susan Groshen, Fabio Penna, Patrizio Odetti, Laura Perin, Peter S. Conti, Yuji Ikeno, Brian K. Kennedy, Pinchas Cohen, Todd E. Morgan, Tanya B. Dorff, and Valter D. Longo. A periodic diet that mimics fasting promotes multi-system regeneration, enhanced cognitive performance, and healthspan. *Cell Metabolism*, 22 (1):86–99, July 2015. ISSN 1550-4131. doi: 10.1016/j.cmet.2015.05.012. URL http://dx.doi.org/10.1016/j.cmet.2015.05.012.

[63] Claudio Vernieri, Giovanni Fucà, Francesca Ligorio, Veronica Huber, Andrea Vingiani, Fabio Iannelli, Alessandra Raimondi, Darawan Rinchai, Gianmaria Frigè, Antonino Belfiore, Luca Lalli, Claudia Chiodoni, Valeria Cancila, Federica Zanardi, Arta Ajazi, Salvatore Cortellino, Viviana Vallacchi, Paola Squarcina, Agata Cova, Samantha Pesce, Paola Frati, Raghvendra Mall, Paola Antonia Corsetto, Angela Maria Rizzo, Cristina Ferraris, Secondo Folli, Marina Chiara Garassino, Giuseppe Capri, Giulia Bianchi, Mario Paolo Colombo, Saverio Minucci, Marco Foiani, Valter Daniel Longo, Giovanni Apolone, Valter Torri, Giancarlo Pruneri, Davide Bedognetti, Licia Rivoltini, and Filippo de Braud. Fasting-mimicking diet is safe and reshapes metabolism and antitumor immunity in patients with cancer. *Cancer Discovery*, 12(1):90–107, November 2021. ISSN 2159-8290. doi:

10.1158/2159-8290.cd-21-0030. URL http://dx.doi.org/10.1158/2159-8290.CD-21-0030.

[64] Lei Wang, Yu-jie Wang, Rong Wang, Fu-lian Gong, Yu-huan Shi, Sheng-nan Li, Pan-pan Chen, and Yong-fang Yuan. Fasting mimicking diet inhibits tumor-associated macrophage survival and pro-tumor function in hypoxia: implications for combination therapy with anti-angiogenic agent. *Journal of Translational Medicine*, 21(1), October 2023. ISSN 1479-5876. doi: 10.1186/s12967-023-04577-7. URL http://dx.doi.org/10.1186/s12967-023-04577-7.

[65] Giulia Salvadori, Federica Zanardi, Fabio Iannelli, Riccardo Lobefaro, Claudio Vernieri, and Valter D. Longo. Fasting-mimicking diet blocks triple-negative breast cancer and cancer stem cell escape. *Cell Metabolism*, 33(11):2247–2259.e6, November 2021. ISSN 1550-4131. doi: 10.1016/j.cmet.2021.10.008. URL http://dx.doi.org/10.1016/j.cmet.2021.10.008.

[66] Paolo Contiero, Franco Berrino, Giovanna Tagliabue, Antonio Mastroianni, Maria Gaetana Di Mauro, Sabrina Fabiano, Monica Annulli, and Paola Muti. Fasting blood glucose and long-term prognosis of non-metastatic breast cancer: a cohort study. *Breast Cancer Research and Treatment*, 138(3):951–959, April 2013. ISSN 1573-7217. doi: 10.1007/s10549-013-2519-9. URL http://dx.doi.org/10.1007/s10549-013-2519-9.

[67] Stefanie de Groot, Rieneke T. Lugtenberg, Danielle Cohen, Marij J. P. Welters, Ilina Ehsan, Maaike P. G. Vreeswijk, Vincent T. H. B. M. Smit, Hiltje de Graaf, Joan B. Heijns, Johanneke E. A. Portielje, Agnes J. van de Wouw, Alex L. T. Imholz, Lonneke W. Kessels, Suzan Vrijaldenhoven, Arnold Baars, Elma Meershoek-Klein Kranenbarg, Marjolijn Duijm-de Carpentier, Hein Putter, Jacobus J. M. van der Hoeven, Johan W. R. Nortier, Valter D. Longo, Hanno Pijl, Judith R. Kroep, Hiltje de Graaf, Joan B. Heijns, Johanneke E. A. Portielje, Agnes J. van de Wouw, Alex L. T. Imholz, Lonneke W. Kessels, Suzan Vrijaldenhoven, Arnold Baars, Emine Göker, Anke J. M. Pas, Aafke H. Honkoop, A. Elise van Leeuwen-Stok, and Judith R. Kroep. Fasting mimicking diet as an adjunct toneoadjuvant chemotherapy for breast cancer in the multicentre randomized phase 2 direct trial. *Nature Communications*, 11(1), June 2020. ISSN 2041-1723. doi: 10.1038/s41467-020-16138-3. URL http://dx.doi.org/10.1038/s41467-020-16138-3.

[68] Francesca Ligorio, Riccardo Lobefaro, Giovanni Fucà, Leonardo Provenzano, Lucrezia Zanenga, Vincenzo Nasca, Caterina Sposetti, Giulia Salvadori, Angela Ficchì, Andrea Franza, Antonia Martinetti, Elisa Sottotetti, Barbara Formisano, Cather-

ine Depretto, Gianfranco Scaperrotta, Antonino Belfiore, Andrea Vingiani, Cristina Ferraris, Giancarlo Pruneri, Filippo de Braud, and Claudio Vernieri. Adding fasting-mimicking diet to first-line carboplatin-based chemotherapy is associated with better overall survival in advanced triple-negative breast cancer patients: A subanalysis of the <scp>nct03340935</scp> trial. *International Journal of Cancer*, 154(1):114–123, August 2023. ISSN 1097-0215. doi: 10.1002/ijc.34701. URL http://dx.doi.org/10.1002/ijc.34701.

[69] Marianne I. Martić-Kehl, Roger Schibli, and P. August Schubiger. Can animal data predict human outcome? problems and pitfalls of translational animal research. *European Journal of Nuclear Medicine and Molecular Imaging*, 39(9):1492–1496, July 2012. ISSN 1619-7089. doi: 10.1007/s00259-012-2175-z. URL http://dx.doi.org/10.1007/s00259-012-2175-z.

[70] Vijay K Singh and Thomas M Seed. How necessary are animal models for modern drug discovery? *Expert Opinion on Drug Discovery*, 16(12):1391–1397, September 2021. ISSN 1746-045X. doi: 10.1080/17460441.2021.1972255. URL http://dx.doi.org/10.1080/17460441.2021.1972255.

[71] Zhitao Li, Wubin Zheng, Hanjin Wang, Ye Cheng, Yijiao Fang, Fan Wu, Guoqiang Sun, Guangshun Sun, Chengyu Lv, and Bingqing Hui. Application of animal models in cancer research: Recent progress and future prospects. *Cancer Management and Research*, Volume 13:2455–2475, March 2021. ISSN 1179-1322. doi: 10.2147/cmar.s302565. URL http://dx.doi.org/10.2147/CMAR.S302565.

[72] John A. Hickman, Ralph Graeser, Ronald de Hoogt, Suzana Vidic, Catarina Brito, Matthias Gutekunst, Heiko van der Kuip, and IMI PREDECT consortium. Three-dimensional models of cancer for pharmacology and cancer cell biology: Capturing tumor complexity in vitro/ex vivo. *Biotechnology Journal*, 9(9): 1115–1128, September 2014. ISSN 1860-7314. doi: 10.1002/biot.201300492. URL http://dx.doi.org/10.1002/biot.201300492.

[73] Xian Xu, Mary C. Farach-Carson, and Xinqiao Jia. Three-dimensional in vitro tumor models for cancer research and drug evaluation. *Biotechnology Advances*, 32 (7):1256–1268, November 2014. ISSN 0734-9750. doi: 10.1016/j.biotechadv.2014.07.009. URL http://dx.doi.org/10.1016/j.biotechadv.2014.07.009.

[74] Mélanie A. G. Barbosa, Cristina P. R. Xavier, Rúben F. Pereira, Vilma Petrikaitė, and M. Helena Vasconcelos. 3d cell culture models as recapitulators of the tumor microenvironment for the screening of anti-cancer drugs. *Cancers*, 14(1):

190, December 2021. ISSN 2072-6694. doi: 10.3390/cancers14010190. URL http://dx.doi.org/10.3390/cancers14010190.

[75] Melica Nourmoussavi Brodeur, Kayla Simeone, Kim Leclerc-Deslauniers, Hubert Fleury, Euridice Carmona, Diane M. Provencher, and Anne-Marie Mes-Masson. Carboplatin response in preclinical models for ovarian cancer: comparison of 2d monolayers, spheroids, ex vivo tumors and in vivo models. *Scientific Reports*, 11 (1), September 2021. ISSN 2045-2322. doi: 10.1038/s41598-021-97434-w. URL http://dx.doi.org/10.1038/s41598-021-97434-w.

[76] Fabrizio Fontana, Monica Marzagalli, Michele Sommariva, Nicoletta Gagliano, and Patrizia Limonta. In vitro 3d cultures to model the tumor microenvironment. *Cancers*, 13(12):2970, June 2021. ISSN 2072-6694. doi: 10.3390/cancers13122970. URL http://dx.doi.org/10.3390/cancers13122970.

[77] Akram Salami Ghaleh, Sepideh Saghati, Reza Rahbarghazi, Ayla Hassani, Leila Shafiei Kaleybar, Mohammad Hossein Geranmayeh, Mehdi Hassanpour, Jafar Rezaie, and Hossein Soltanzadeh. Static and dynamic culture of human endothelial cells encapsulated inside alginate-gelatin microspheres. *Microvascular Research*, 137:104174, September 2021. ISSN 0026-2862. doi: 10.1016/j.mvr.2021.104174. URL http://dx.doi.org/10.1016/j.mvr.2021.104174.

[78] Rishab Driver and Shweta Mishra. Organ-on-a-chip technology: An in-depth review of recent advancements and future of whole body-on-chip. *BioChip Journal*, 17(1): 1–23, October 2022. ISSN 2092-7843. doi: 10.1007/s13206-022-00087-8. URL http://dx.doi.org/10.1007/s13206-022-00087-8.

[79] John P Wikswo. The relevance and potential roles of microphysiological systems in biology and medicine. *Experimental Biology and Medicine*, 239(9):1061–1072, September 2014. ISSN 1535-3699. doi: 10.1177/1535370214542068. URL http://dx.doi.org/10.1177/1535370214542068.

[80] Aleksei P. Iakovlev, Alexander S. Erofeev, and Petr V. Gorelkin. Novel pumping methods for microfluidic devices: A comprehensive review. *Biosensors*, 12(11): 956, November 2022. ISSN 2079-6374. doi: 10.3390/bios12110956. URL http://dx.doi.org/10.3390/BIOS12110956.

[81] Mohana Marimuthu and Sanghyo Kim. Pumpless steady-flow microfluidic chip for cell culture. *Analytical Biochemistry*, 437(2):161–163, June 2013. ISSN 0003-2697. doi: 10.1016/j.ab.2013.02.007. URL http://dx.doi.org/10.1016/J.AB.2013.02.007.

[82] Christian Lohasz, Nassim Rousset, Kasper Renggli, Andreas Hierlemann, and Olivier Frey. Scalable microfluidic platform for flexible configuration of and experiments with microtissue multiorgan models. *SLAS Technology*, 24(1):79–95, February 2019. ISSN 2472-6303. doi: 10.1177/2472630318802582. URL http://dx.doi.org/10.1177/2472630318802582.

[83] Stefan Schneider, Marvin Bubeck, Julia Rogal, Huub J. Weener, Cristhian Rojas, Martin Weiss, Michael Heymann, Andries D. van der Meer, and Peter Loskill. Peristaltic on-chip pump for tunable media circulation and whole blood perfusion in pdms-free organ-on-chip and organ-disc systems. *Lab on a Chip*, 21 (20):3963–3978, 2021. ISSN 1473-0189. doi: 10.1039/d1lc00494h. URL http://dx.doi.org/10.1039/D1LC00494H.

[84] Jannick Theobald, Ali Ghanem, Patrick Wallisch, Amin A. Banaeiyan, Miguel A. Andrade-Navarro, Katerina Taškova, Manuela Haltmeier, Andreas Kurtz, Holger Becker, Stefanie Reuter, Ralf Mrowka, Xinlai Cheng, and Stefan Wölfl. Liver-kidney-on-chip to study toxicity of drug metabolites. *ACS Biomaterials Science & Engineering*, 4(1):78–89, December 2017. ISSN 2373-9878. doi: 10.1021/acsbiomaterials.7b00417. URL http://dx.doi.org/10.1021/ACSBIOMATERIALS.7B00417.

[85] Jonathan W. Song, Julien Daubriac, Janet M. Tse, Despina Bazou, and Lance L. Munn. Rhoa mediates flow-induced endothelial sprouting in a 3-d tissue analogue of angiogenesis. *Lab on a Chip*, 12(23):5000, 2012. ISSN 1473-0189. doi: 10.1039/c2lc40389g. URL http://dx.doi.org/10.1039/C2LC40389G.

[86] Job Komen, Sanne M. van Neerven, Albert van den Berg, Louis Vermeulen, and Andries D. van der Meer. Mimicking and surpassing the xenograft model with cancer-on-chip technology. *eBioMedicine*, 66:103303, April 2021. ISSN 2352-3964. doi: 10.1016/j.ebiom.2021.103303. URL http://dx.doi.org/10.1016/j.ebiom.2021.103303.

[87] Xingxing Liu, Qiuping Su, Xiaoyu Zhang, Wenjian Yang, Junhua Ning, Kangle Jia, Jinlan Xin, Huanling Li, Longfei Yu, Yuheng Liao, and Diming Zhang. Recent advances of organ-on-a-chip in cancer modeling research. *Biosensors*, 12(11):1045, November 2022. ISSN 2079-6374. doi: 10.3390/bios12111045. URL http://dx.doi.org/10.3390/bios12111045.

[88] Shuai Liu, Wei Yang, Yunlei Li, and Changqing Sun. Fetal bovine serum, an important factor affecting the reproducibility of cell experiments. *Scientific Reports*,

13(1), February 2023. ISSN 2045-2322. doi: 10.1038/s41598-023-29060-7. URL http://dx.doi.org/10.1038/s41598-023-29060-7.

[89] Chiara Vitale, Monica Marzagalli, Silvia Scaglione, Alessandra Dondero, Cristina Bottino, and Roberta Castriconi. Tumor microenvironment and hydrogel-based 3d cancer models for in vitro testing immunotherapies. *Cancers*, 14(4):1013, February 2022. ISSN 2072-6694. doi: 10.3390/cancers14041013. URL http://dx.doi.org/10.3390/CANCERS14041013.

[90] Marta Cavo, Marco Fato, Leonardo Peñuela, Francesco Beltrame, Roberto Raiteri, and Silvia Scaglione. Microenvironment complexity and matrix stiffness regulate breast cancer cell activity in a 3d in vitro model. *Scientific Reports*, 6(1), October 2016. ISSN 2045-2322. doi: 10.1038/srep35367. URL http://dx.doi.org/10.1038/srep35367.

[91] Amit Khurana and Chandraiah Godugu. *Alginate-Based Three-Dimensional In Vitro Tumor Models: A Better Alternative to Current Two-Dimensional Cell Culture Models*, page 157–183. Springer Singapore, November 2017. ISBN 9789811069109. doi: 10.1007/978-981-10-6910-9_6. URL http://dx.doi.org/10.1007/978-981-10-6910-9_6.

[92] Maitham A. Khajah, Sarah Khushaish, and Yunus A. Luqmani. Glucose deprivation reduces proliferation and motility, and enhances the anti-proliferative effects of paclitaxel and doxorubicin in breast cell lines in vitro. *PLOS ONE*, 17(8): e0272449, August 2022. ISSN 1932-6203. doi: 10.1371/journal.pone.0272449. URL http://dx.doi.org/10.1371/JOURNAL.PONE.0272449.

[93] Miaomiao Li, Wenjing Huang, Yuan Zhang, Yue Du, Shan Zhao, Longhao Wang, Yaxin Sun, Beibei Sha, Jie Yan, Yangcheng Ma, Jinlu Tang, Jianxiang Shi, Pei Li, Lijun Jia, Tao Hu, and Ping Chen. Glucose deprivation triggers dcaf1-mediated inactivation of rheb-mtorc1 and promotes cancer cell survival. *Cell Death & Disease*, 15(6), June 2024. ISSN 2041-4889. doi: 10.1038/s41419-024-06808-1. URL http://dx.doi.org/10.1038/s41419-024-06808-1.

[94] C. Curtin, J.C. Nolan, R. Conlon, L. Deneweth, C. Gallagher, Y.J. Tan, B.L. Cavanagh, A.Z. Asraf, H. Harvey, S. Miller-Delaney, J. Shohet, I. Bray, F.J. O'Brien, R.L. Stallings, and O. Piskareva. A physiologically relevant 3d collagen-based scaffold–neuroblastoma cell system exhibits chemosensitivity similar to orthotopic xenograft models. *Acta Biomaterialia*, 70:84–97, April 2018. ISSN 1742-7061.

doi: 10.1016/j.actbio.2018.02.004. URL http://dx.doi.org/10.1016/J.ACTBIO.2018.02.004.

[95] Eva Lhuissier, Céline Bazille, Juliette Aury-Landas, Nicolas Girard, Julien Pontin, Martine Boittin, Karim Boumediene, and Catherine Baugé. Identification of an easy to use 3d culture model to investigate invasion and anticancer drug response in chondrosarcomas. *BMC Cancer*, 17(1), July 2017. ISSN 1471-2407. doi: 10.1186/s12885-017-3478-z. URL http://dx.doi.org/10.1186/s12885-017-3478-z.

[96] Kristin Stock, Marta F. Estrada, Suzana Vidic, Kjersti Gjerde, Albin Rudisch, Vítor E. Santo, Michaël Barbier, Sami Blom, Sharath C. Arundkar, Irwin Selvam, Annika Osswald, Yan Stein, Sylvia Gruenewald, Catarina Brito, Wytske van Weerden, Varda Rotter, Erwin Boghaert, Moshe Oren, Wolfgang Sommergruber, Yolanda Chong, Ronald de Hoogt, and Ralph Graeser. Capturing tumor complexity in vitro: Comparative analysis of 2d and 3d tumor models for drug discovery. *Scientific Reports*, 6(1), July 2016. ISSN 2045-2322. doi: 10.1038/srep28951. URL http://dx.doi.org/10.1038/srep28951.

[97] Maia Al-Masri, Karina Paliotti, Raymond Tran, Ruba Halaoui, Virginie Lelarge, Sudipa Chatterjee, Li-Ting Wang, Christopher Moraes, and Luke McCaffrey. Architectural control of metabolic plasticity in epithelial cancer cells. *Communications Biology*, 4(1), March 2021. ISSN 2399-3642. doi: 10.1038/s42003-021-01899-4. URL http://dx.doi.org/10.1038/S42003-021-01899-4.

[98] Edward Henry Mathews, B. André Stander, Annie M. Joubert, and Leon Liebenberg. Tumor cell culture survival following glucose and glutamine deprivation at typical physiological concentrations. *Nutrition*, 30(2):218–227, February 2014. ISSN 0899-9007. doi: 10.1016/j.nut.2013.07.024. URL http://dx.doi.org/10.1016/j.nut.2013.07.024.

[99] Anna Priebe, Lijun Tan, Heather Wahl, Angela Kueck, Gong He, Roland Kwok, Anthony Opipari, and J. Rebecca Liu. Glucose deprivation activates ampk and induces cell death through modulation of akt in ovarian cancer cells. *Gynecologic Oncology*, 122(2):389–395, August 2011. ISSN 0090-8258. doi: 10.1016/j.ygyno.2011.04.024. URL http://dx.doi.org/10.1016/J.YGYNO.2011.04.024.

[100] Hao Wu, Zonghui Ding, Danqing Hu, Feifei Sun, Chunyan Dai, Jiansheng Xie, and Xun Hu. Central role of lactic acidosis in cancer cell resistance to glucose deprivation-induced cell death. *The Journal of Pathology*, 227(2):189–199, February

2012. ISSN 1096-9896. doi: 10.1002/path.3978. URL http://dx.doi.org/10.1002/path.3978.

[101] Gregg L Semenza. Hif-1: upstream and downstream of cancer metabolism. *Current Opinion in Genetics & Development*, 20(1):51–56, February 2010. ISSN 0959-437X. doi: 10.1016/j.gde.2009.10.009. URL http://dx.doi.org/10.1016/J.GDE.2009.10.009.

[102] Domenico Ribatti and Angelo Vacca. The role of microenvironment in tumor angiogenesis. *Genes & Nutrition*, 3(1):29–34, February 2008. ISSN 1865-3499. doi: 10.1007/s12263-008-0076-3. URL http://dx.doi.org/10.1007/S12263-008-0076-3.

[103] Yutaka Yamamoto, Mutsuko Ibusuki, Yasuhiro Okumura, Teru Kawasoe, Kazuharu Kai, Kenichi Iyama, and Hirotaka Iwase. Hypoxia-inducible factor 1α is closely linked to an aggressive phenotype in breast cancer. *Breast Cancer Research and Treatment*, 110(3):465–475, September 2007. ISSN 1573-7217. doi: 10.1007/s10549-007-9742-1. URL http://dx.doi.org/10.1007/S10549-007-9742-1.

[104] ARATA NISHIMOTO, NARUJI KUGIMIYA, TOHRU HOSOYAMA, TADAHIKO ENOKI, TAO-SHENG LI, and KIMIKAZU HAMANO. Hif-1α activation under glucose deprivation plays a central role in the acquisition of anti-apoptosis in human colon cancer cells. *International Journal of Oncology*, 44(6):2077–2084, April 2014. ISSN 1791-2423. doi: 10.3892/ijo.2014.2367. URL http://dx.doi.org/10.3892/IJO.2014.2367.

[105] Peter Rossow, Michael S. Radeos, and Harold Amos. Metabolic effects of glucose starvation in animal cell cultures. *Archives of Biochemistry and Biophysics*, 168(2):520–524, June 1975. ISSN 0003-9861. doi: 10.1016/0003-9861(75)90282-9. URL http://dx.doi.org/10.1016/0003-9861(75)90282-9.

[106] J L Su, K Ma, C P Zhang, and Xiaobing Fu. Effect of human decidua mesenchymal stem cells-derived exosomes on the function of high glucose-induced senescent human dermal fibroblasts and its possible mechanism. *Zhonghua Shao Shang Yu Chuang Mian Xiu Fu Za Zhi*, 38(2):170–183, February 2022.

[107] Helena C. Oft, Dennis W. Simon, and Dandan Sun. New insights into metabolism dysregulation after tbi. *Journal of Neuroinflammation*, 21(1), July 2024. ISSN 1742-2094. doi: 10.1186/s12974-024-03177-6. URL http://dx.doi.org/10.1186/S12974-024-03177-6.

[108] Alessandra Marrella. 3d fluid-dynamic ovarian cancer model resembling systemic

drug administration for efficacy assay. *ALTEX*, 2020. ISSN 1868-596X. doi: 10.14573/altex.2003131. URL http://dx.doi.org/10.14573/altex.2003131.

[109] Praseetha Prabhakaran, Foteini Hassiotou, Pilar Blancafort, and Luis Filgueira. Cisplatin induces differentiation of breast cancer cells. *Frontiers in Oncology*, 3, 2013. ISSN 2234-943X. doi: 10.3389/fonc.2013.00134. URL http://dx.doi.org/10.3389/FONC.2013.00134.

[110] Elisa Rossini, Valentina Bosatta, Andrea Abate, Martina Fragni, Valentina Salvi, Ram Manohar Basnet, Daniela Zizioli, Daniela Bosisio, Giovanna Piovani, Francesca Valcamonico, Giuseppe Mirabella, Alfredo Berruti, Maurizio Memo, and Sandra Sigala. Cisplatin cytotoxicity in human testicular germ cell tumor cell lines is enhanced by the cdk4/6 inhibitor palbociclib. *Clinical Genitourinary Cancer*, 19(4): 316–324, August 2021. ISSN 1558-7673. doi: 10.1016/j.clgc.2021.01.006. URL http://dx.doi.org/10.1016/J.CLGC.2021.01.006.

[111] Paula Engbers-Buijtenhuijs, Laura Buttafoco, Andre A. Poot, Piet J. Dijkstra, Rob A.I. de Vos, Lotus M.Th. Sterk, Rob H. Geelkerken, Istvan Vermes, and Jan Feijen. Biological characterisation of vascular grafts cultured in a bioreactor. *Biomaterials*, 27(11):2390–2397, April 2006. ISSN 0142-9612. doi: 10.1016/j.biomaterials.2005.10.016. URL http://dx.doi.org/10.1016/J.BIOMATERIALS.2005.10.016.

[112] Yesl Jun, JaeSeo Lee, Seongkyun Choi, Ji Hun Yang, Maike Sander, Seok Chung, and Sang-Hoon Lee. In vivo–mimicking microfluidic perfusion culture of pancreatic islet spheroids. *Science Advances*, 5(11), November 2019. ISSN 2375-2548. doi: 10.1126/sciadv.aax4520. URL http://dx.doi.org/10.1126/SCIADV.AAX4520.

[113] Karolina Penderecka, Matthew Ibbs, Apolonia Kaluzna, Anna Lewandowska, Andrzej Marszalek, Andrzej Mackiewicz, and Hanna Dams-Kozlowska. Implementation of a dynamic culture condition to the heterotypic 3d breast cancer model. *Journal of Biomedical Materials Research Part B: Applied Biomaterials*, 108(4): 1186–1197, August 2019. ISSN 1552-4981. doi: 10.1002/jbm.b.34468. URL http://dx.doi.org/10.1002/JBM.B.34468.

[114] ElShaddai Z. White, Nakea M. Pennant, Jada R. Carter, Ohuod Hawsawi, Valerie Odero-Marah, and Cimona V. Hinton. Serum deprivation initiates adaptation and survival to oxidative stress in prostate cancer cells. *Scientific Reports*, 10(1), July 2020. ISSN 2045-2322. doi: 10.1038/s41598-020-68668-x. URL http://dx.doi.org/10.1038/S41598-020-68668-X.

[115] Le Yu, Chunping Gu, Desheng Zhong, Lili Shi, Yi Kong, Zhitao Zhou, and Shuwen

Liu. Induction of autophagy counteracts the anticancer effect of cisplatin in human esophageal cancer cells with acquired drug resistance. *Cancer Letters*, 355(1):34–45, December 2014. ISSN 0304-3835. doi: 10.1016/j.canlet.2014.09.020. URL http://dx.doi.org/10.1016/J.CANLET.2014.09.020.

[116] S Koch, F Mayer, F Honecker, M Schittenhelm, and C Bokemeyer. Efficacy of cytotoxic agents used in the treatment of testicular germ cell tumours under normoxic and hypoxic conditions in vitro. *British Journal of Cancer*, 89(11): 2133–2139, November 2003. ISSN 1532-1827. doi: 10.1038/sj.bjc.6601375. URL http://dx.doi.org/10.1038/SJ.BJC.6601375.

[117] Tijana Stanković, Teodora Ranđelović, Miodrag Dragoj, Sonja Stojković Burić, Luis Fernández, Ignacio Ochoa, Victor M. Pérez-García, and Milica Pešić. In vitro biomimetic models for glioblastoma-a promising tool for drug response studies. *Drug Resistance Updates*, 55:100753, March 2021. ISSN 1368-7646. doi: 10.1016/j.drup.2021.100753. URL http://dx.doi.org/10.1016/J.DRUP.2021.100753.

[118] Meilin Sun, Jinwei Zhang, Wenzhu Fu, Tingting Xuanyuan, and Wenming Liu. Facile construction of a 3d tumor model with multiple biomimetic characteristics using a micropatterned chip for large-scale chemotherapy investigation. *Lab on a Chip*, 23(9):2161–2174, 2023. ISSN 1473-0189. doi: 10.1039/d3lc00009e. URL http://dx.doi.org/10.1039/D3LC00009E.

[119] Roberta Buono and Valter D. Longo. Starvation, stress resistance, and cancer. *Trends in Endocrinology & Metabolism*, 29(4):271–280, April 2018. ISSN 1043-2760. doi: 10.1016/j.tem.2018.01.008. URL http://dx.doi.org/10.1016/j.tem.2018.01.008.

[120] Stefano Di Biase, Changhan Lee, Sebastian Brandhorst, Brianna Manes, Roberta Buono, Chia-Wei Cheng, Mafalda Cacciottolo, Alejandro Martin-Montalvo, Rafael de Cabo, Min Wei, Todd E. Morgan, and Valter D. Longo. Fasting-mimicking diet reduces ho-1 to promote t cell-mediated tumor cytotoxicity. *Cancer Cell*, 30 (1):136–146, July 2016. ISSN 1535-6108. doi: 10.1016/j.ccell.2016.06.005. URL http://dx.doi.org/10.1016/j.ccell.2016.06.005.

[121] Alessio Nencioni, Irene Caffa, Salvatore Cortellino, and Valter D. Longo. Fasting and cancer: molecular mechanisms and clinical application. *Nature Reviews Cancer*, 18(11):707–719, October 2018. ISSN 1474-1768. doi: 10.1038/s41568-018-0061-0. URL http://dx.doi.org/10.1038/s41568-018-0061-0.

List of Figures

Acknowledgements

In primo luogo desidero esprimere la mia gratitudine ai i miei relatori Gianluca Ciardelli, Silvia Scaglione per la loro guida preziosa, il supporto e la pazienza costanti dimostrati durante l'intero sviluppo di tesi. I vostri consigli così come la vostra esperienza sono stati determinanti per il raggiungimento di questo obbiettivo nonché fonte di ispirazione per crescita accademica e professionale.

Ringrazio inoltre Elisabetta Palamà, figura di riferimento e costante fonte di conoscenza ed esperienza. Grazie a te ho mosso i primi passi in laboratorio, mi hai condotto all'interno di un mondo a me poco conosciuto. Mi hai fornito sapientemente le basi e gli strumenti necessari per poter agire responsabilmente e consapevolmente in autonomia.

Un sentito ringraziamento va a React4Life, l'azienda che ha deciso di credere in me concedendomi l'onore di condurre il mio progetto di tesi all'interno della sua realtà. Vorrei ringraziare in particolar modo tutte le persone all'interno della stessa che ne costituiscono anima e corpo. A partire da Maurizio e Silvia, che hanno fatto della propria passione per la ricerca ed il progresso un lavoro. Siete a mio parere un modello esemplare di ispirazione per tutte le giovani menti italiane e non solo. Il ringraziamento va esteso anche a tutti i restanti colleghi che hanno reso questi mesi un'occasione di crescita personale e professionale e che non hanno esitato ad aiutarmi e sostenermi nei miei momenti di difficoltà.

Un ringraziamento importante va alla mia famiglia. A mia madre, mio padre e mia sorella per avermi supportato ed accompagnato lungo tutto questo percorso. Con il vostro sostegno e aiuto morale, e non solo, è stato per me possibile raggiungere questo traguardo. Durante questi anni di studio lontano da casa, siete comunque riusciti a farmi sentire vicino. Tutte le videochiamate o foto vi assicuro che, nonostante i non pochi chilometri, hanno aiutato a distrarmi dalla distanza da casa. Mi avete fatto sentire vicino e partecipe, nei limiti del possibile, alla vita in famiglia, in casa tra voi, familiari e parenti vari. Ciò è stato senz'altro importante in non poche occasioni. È inutile nasconderlo, vivere indipendente con i propri spazi e tempi può essere bello quanto vuoi ma alla fine casa è sempre casa. Inoltre, sento il dovere e il piacere di ringraziarvi per tutto il sostegno

economico in questi anni di studio. Sono consapevole del valore di tutti i vostri sacrifici e vi sono enormemente riconoscente per non avermi fatto mancare mai nulla.

Un grazie speciale a Mari che mi ha accompagnato in questi anni. La persona con cui ho condiviso un'importante parte della mia vita. Mi hai sostenuto in tutti i momenti di maggiore difficoltà. Mi hai insegnato cosa significa dedicarsi profondamente a qualcuno, rendersi sempre disponibili all'aiuto.

Vorrei ringraziare anche tutti i miei parenti e familiari, tra cui mia nonna Ada e nonno Armando. Caro nonno, grazie per tutti i tuoi "Cosa vuoi fare da grande?". Da piccolo questa domanda mi entusiasmava e spaventava al tempo stesso. Oggi direi che la risposta è un tantino più chiara.

Grazie a Gianmatteo e Melo. Ci siamo incontrati per caso, abbiamo condiviso una prima tappa insieme per poi separarci e ritrovarci nuovamente a Torino. A conti fatti, direi che non è più un caso.

Ringrazio anche gli amici e colleghi di Torino con cui ho avuto il piacere di condividere bei momenti tra studio e serate.

Un grazie a tutti i miei amici di GIÙ che nonostante la distanza sono sempre rimasti con me.

Un grazie speciale anche a Piuma e Lara. Sempre e comunque felici di rivedermi.

Ai miei capelli, che ancora (per poco) resistono, dopo tutto.